



Sedimentary dynamics of the shallow water facies of Puncoviscana basin in the Neoproterozoic – Early Cambrian transition, NW Argentina

Dinámica de la sedimentación de las facies someras de la cuenca Puncoviscana en la transición Neoproterozoico-Cámbrico inferior, NO de Argentina

Vanina L. LÓPEZ^{1*} , Walter J. CHILIGUAY², María de las M. ORTEGA PÉREZ³ , Miguel B. AZAREVICH⁴

¹ Centro de Estudios Geológicos Andinos (CEGA), Instituto Superior de Correlación Geológica (INSUGEO), Consejo Nacional de Investigaciones Científicas y Técnicas (CONICET). Universidad Nacional de Salta, Av. Bolivia 5150, CP4400, Salta capital, Argentina.

² Instituto de Geología y Minería de Jujuy, Universidad Nacional de Jujuy.

³ Centro de Estudios Geológicos Andinos (CEGA), Instituto Superior de Correlación Geológica (INSUGEO), Consejo Nacional de Investigaciones Científicas y Técnicas (CONICET), Av. Bolivia 5150, CP4400, Salta capital, Argentina.

⁴ Centro de Estudios Geológicos Andinos (CEGA), Instituto Superior de Correlación Geológica (INSUGEO), Consejo Nacional de Investigaciones Científicas y Técnicas (CONICET), Av. Bolivia 5150, CP4400, Salta capital, Argentina.

* Corresponding author: <vaninalucrecialopez@gmail.com >

Abstract

The Neoproterozoic – Early Cambrian deposits from NW Argentina conform the infilling of Puncoviscana Basin. It represents an elongate, northward opened, foreland marine basin, developed between Amazonia, Antofalla and Pampia Terranes derived from the fragmentation of Rodinia. This basin records sedimentation of basal diamictites, platform and deep marine deposits to the west, followed by cap carbonates that transitionally pass to shallow clastic sequences with few interlayered pyroclastites (Puncoviscana Formation). The shallow marine Puncoviscana Formation contains diagnostic sedimentary structures belonging to intertidal and shallow subtidal environments. Tidal processes are evident due to the presence lenticular to flaser stratification, soft-sediment

► Ref. bibliográfica: Juárez, López, V. L.; Chiliguay, W. J.; Ortega Pérez, M. de las M.; Azarevich, M. B. 2025. "Sedimentary dynamics of the shallow water facies of Puncoviscana basin in the Neoproterozoic – Early Cambrian transition, NW Argentina". *Acta Geológica Lilloana* 36 (1): 51-98. doi: <https://doi.org/10.30550/j.agl/1881>

► Recibido: 27 de diciembre 2023 – Aceptado: 11 de abril 2025

► URL de la revista: <http://actageologica.lillo.org.ar>



► Esta obra está bajo una Licencia Creative Commons Atribución – No Comercial – Sin Obra Derivada 4.0 Internacional.

deformation, tidal rhythmites, herringbones and double-crested ripples. Facies associations resemble shoreface environments along the westmargin, which evolved to tidal flats laterally and upper sequence. The tides flooded over a mesotidal coast, while palaeocurrent analysis display bimodal bipolar and polymodal patterns due to a reversal N-S flood, ebb circulation and littoral drift. From zircon age population sourced to the Puncoviscana Formation, we interpret that subsidence of the basin was episodic. The initial episode of active faulting and subsidence (~570-545 Ma, basal strata of Puncoviscana Formation) was followed by a ~10 Ma-episode of sea level rise (middle Puncoviscana Formation) and a final ~20 Ma-episode that included tectomagmatic activity that progressed to uplift and closure.

Keywords: Puncoviscana Formation, tidal sequence, polymodal paleocurrents, Neoproterozoic – Early Cambrian, NW Argentina.

Resumen

Los depósitos del Neoproterozoico-Cámbrico inferior del NO argentino conforman el relleno de la cuenca Puncoviscana. Ésta representa una cuenca marina de foreland, elongada, abierta hacia el norte, desarrollada entre los terrenos Amazonia, Antofalla y Pampia, que deriva de la fragmentación de Rodinia. La cuenca registra sedimentación de diamictitas basales y depósitos de plataforma hasta marino profundo hacia el este, seguidos de carbonatos post-glaciales y transicionalmente secuencias clásticas someras con intercalaciones piroclásticas (Formación Puncoviscana). La Formación Puncoviscana, marino somera, contiene estructuras sedimentarias diagnósticas de ambientes intermareales y submareales someros. Los procesos mareales son evidenciados a partir de estratificación lenticular a flaser, convoluta, ritmitas mareales, estratificación en hueso de arenque y ondulitas de doble cresta. La asociación de facies corresponde a ambientes de cara de playa a lo largo del margen occidental, que evolucionan hacia planicie mareal lateral y hacia arriba en la secuencia. Las mareas actuaron sobre costas de régimen mesomareal, mientras que el análisis de paleocorrientes demuestra patrones bimodales bipolares, y polimodales debido a flujos reversibles N-S de flujo-reflujo, y deriva litoral. A partir de las poblaciones de edad en zircones aportados a la Formación Puncoviscana, se interpreta que la subsidencia de la cuenca fue episódica. El estadio inicial de fallamiento activo y subsidencia (~570-545 Ma, sección inferior de la Formación Puncoviscana) fue seguido de por un episodio de ~10 Ma de aumento del nivel del mar (sección media de la Formación Puncoviscana) y uno final de ~20 Ma que incluyó actividad tecto-magmática que progresó hacia el levantamiento y cierre de la cuenca.

Palabras clave: Formación Puncoviscana, secuencia mareal, paleocorrientes polimodales, Neoproterozoico – Cámbrico inferior, NO de Argentina.

INTRODUCTION

Over the last three decades, the Neoproterozoic to Early Cambrian deposits from NW Argentina, which conform the Puncoviscana Basin, have been the focus of research towards the comprehension of the palaeoenvironmental settings (Ježek, 1990; Buatois and Mángano, 2004; Aceñolaza and Aceñolaza, 2007; Omarini *et al.*, 2008; López de Azarevich *et al.*, 2010b-c, 2012; Chiliguay *et al.*, 2019), the tectonic processes involved in the Rodinia break-up, and the assembly of western Gondwana (Omarini *et al.*, 1999; Escayola *et al.*, 2011; Rapela *et al.*, 2016). The fragmentation of Rodinia progressed after the third pulse of the Brasiliano Orogeny by ~590-560 Ma (Brito Neves *et al.*, 2014). This generated marine water inundation throughout several pericontinental pathways formed among dispersed landmasses. The sedimentary record in the formed basins show similar features and signatures all around the fragmented Rodinia (Rapela *et al.*, 2016).

Within this paleocontinental framework, Puncoviscana Basin defined a sub-meridian elongate pond bounded by Archean to Neoproterozoic basements: Amazonia Craton and Pampia and Arequipa-Antofalla terranes (Figure 1), and the opening proceeded from a triple junction located near Tarija, Bolivia (Omarini *et al.*, 1999; Ramos, 2008; Aceñolaza and Toselli, 2009). The seawater penetrated from the north, flooding the coasts along the east and west margins, whereas continental flooding ran over glacial to deglacial areas according to the record of the basal sedimentary successions.

The basin infill of Puncoviscana Basin integrates the Lerma Group (Salfity *et al.*, 1976), which began in the Neoproterozoic with coarse diamictites, accompanied by sandstones and siltstones with turbidite arrangements (Figure 2a). Sedimentation continued with postglacial cap carbonate sequences that precipitated along the eastern margin of the basin (Figure 2b). These gradually pass to tidal-influenced deposits of Puncoviscana Formation with Early Cambrian bio-associations (López de Azarevich *et al.*, 2012; Chiliguay *et al.*, 2014, 2016, 2019), into which are interlayered some pyroclastic levels with 545 to 523 Ma U-Pb zircon ages (Escayola *et al.*, 2011). This sedimentary stage in the basin is distributed in both east and west margins (Figure 2c).

A primary interpretation of paleoflow directions for Puncoviscana Formation's sedimentites allowed Ježek (1990) to interpret, in the western border of the basin, turbidite flows with changing directions of turbulent currents in the frontal lobes. However, no evidence of turbidite facies was found in further studies in Puncoviscana Formation (López de Azarevich, 2010; López de Azarevich *et al.*, 2010a). Furthermore, the multidirectional paleocurrents recognized from shallow water sedimentary structures indicate marine settings affected by tides and littoral currents (López de Azarevich and Azarevich, 2015b).

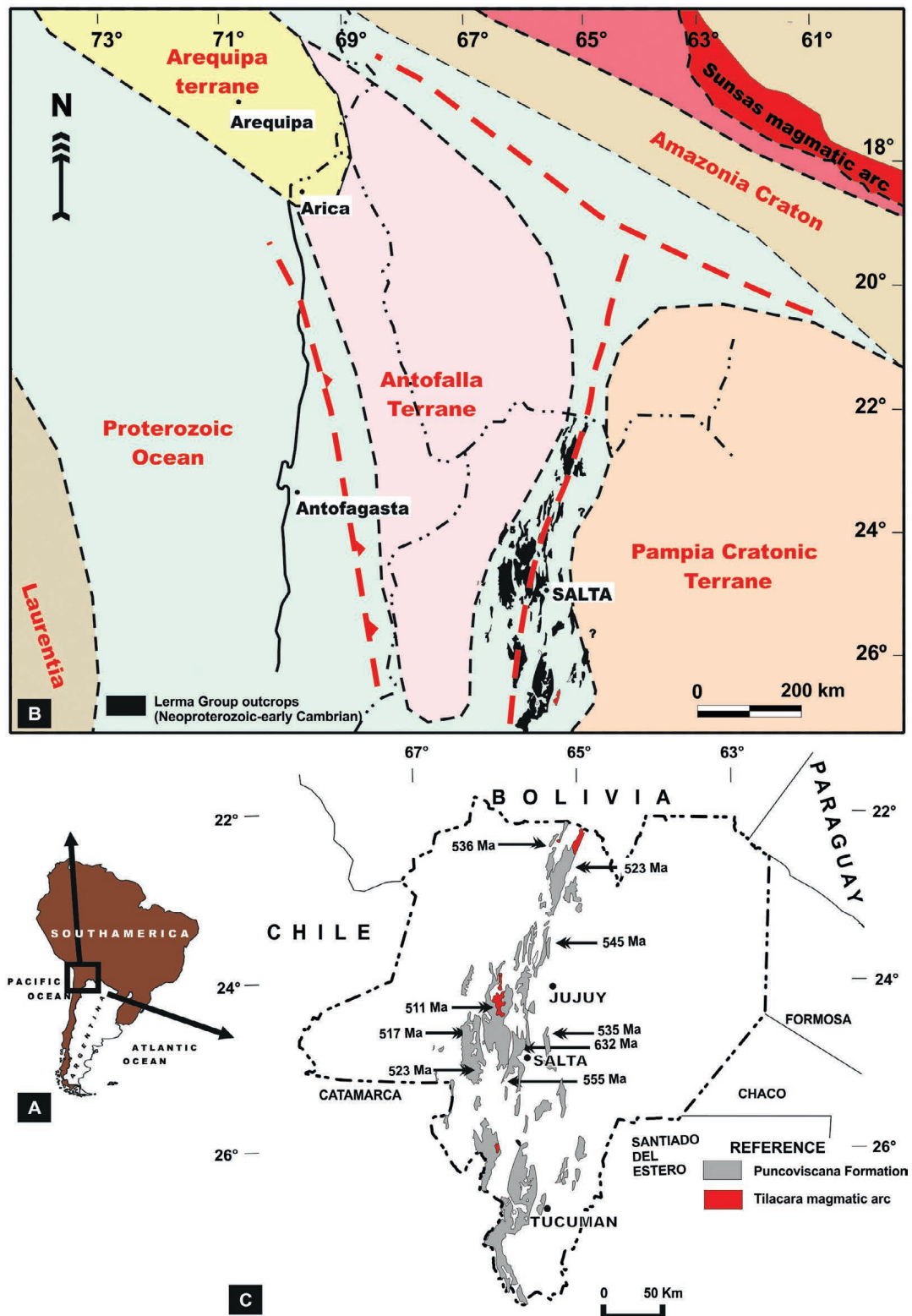


Figure 1. Location and configuration of Puncoviscana Basin. a. Location of the study area. b. Paleogeographic configuration of Rodinia Supercontinent breakup and generation of the Puncoviscana Basin between Pampia, Antofalla and Amazonia. Modified from data of Omarini *et al.* (1999), Ramos (2008), Aceñolaza and Toselli (2009). c. Distribution of Puncoviscana Formation outcrops and Tilcara Arc intrusives. Zircon U-Pb ages compiled from Aparicio González (2014).

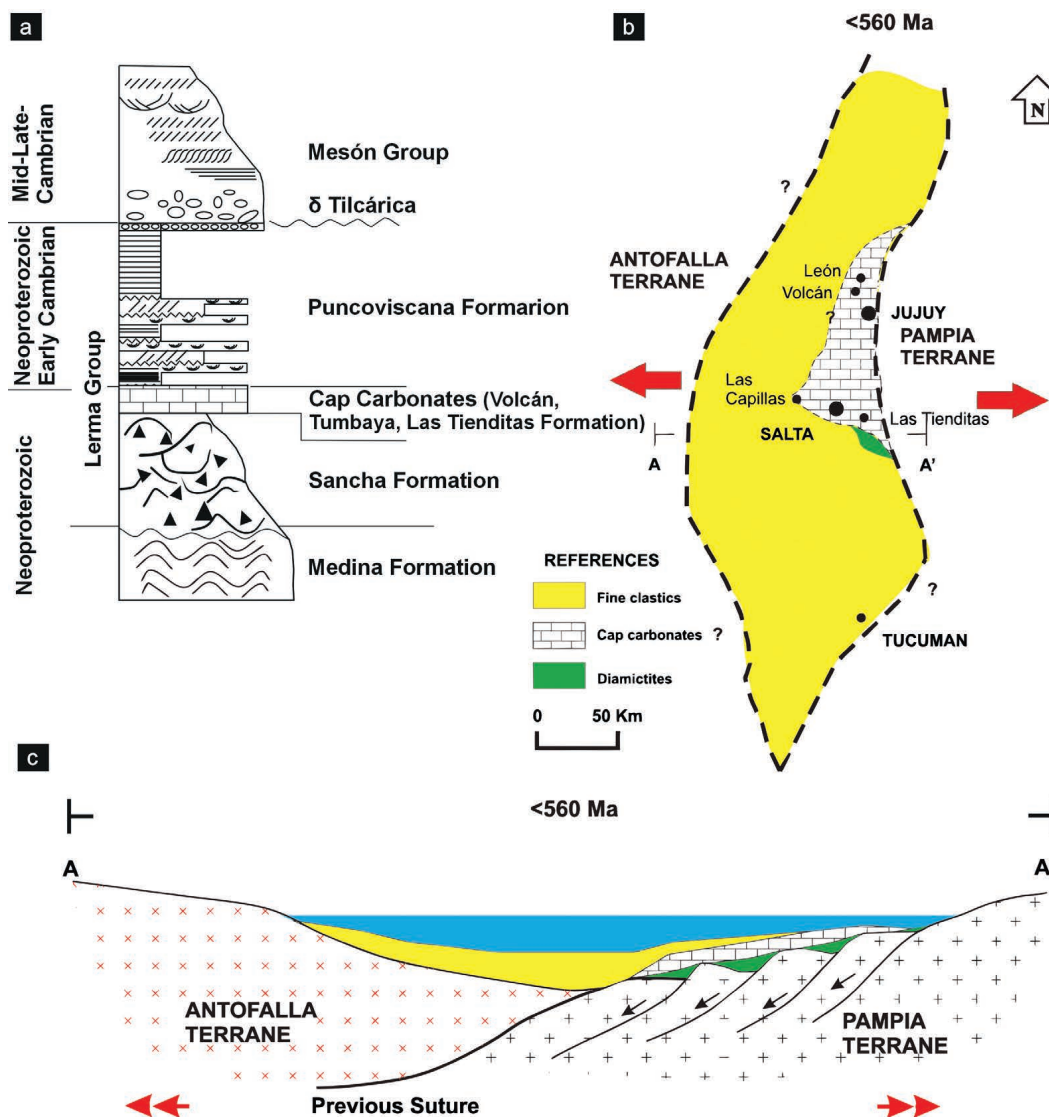


Figure 2. Stratigraphic and geotectonic framework of Puncoviscana Basin. a. Stratigraphic column for Lerma Group (Salfity *et al.*, 1976). b. Opening of Puncoviscana sea, passive margin stage with deposition of Sancha Formation and cap carbonate platforms. c. Emplacement of the older pluton related to the Tilcara Arc (Tipayoc, 550 Ma), active margin stage, beginning of deposition of Puncoviscana Formation with interlayered pyroclastites.

On the other hand, abundant geochronological and geochemical data were used to construct geotectonic models of NW Argentina for Neoproterozoic to Early Cambrian successions. Some interpretations include correlations between the Puncoviscana Basin's deposits and marine deposits from Sierras de Córdoba, central Argentina (Rapela *et al.*, 2016), whereas others interpret the presence of oceanic volcanism accompanying the basin opening and furthermore include this in an evolutionary model (Escayola *et al.*, 2011; Aparicio González, 2014). Even so, there is neither clear evidence supporting the first interpretation, nor ocean crust outcrops of a confirmed Neoproterozoic – Early Cambrian age were found.

Within this context, the purpose of this research is to analyze the geodynamic processes during the Neoproterozoic – Early Cambrian transition involved in the interval from postglacial carbonate to shallow clastic deposition, integrating the geochemical signatures of carbonates and the facies and paleoflow analysis acquired in Puncoviscana Formation along the east and west margins of the basin.

GEOLOGICAL AND GEODYNAMIC FRAMEWORK

Puncoviscana sea opened from the breakup of the Rodinia Supercontinent, a process that started at ~850-740 Ma (Silva *et al.*, 2005; Brito Neves and Fuck, 2013) and ended at ~520 Ma with the final amalgamation of Gondwana (Omarini *et al.*, 1999; Ramos, 2008). Several pericratonic basins developed contemporaneously around the Rodinia fragments from Perú down to Patagonia in South America, with equivalent successions eastwards in Australia and Antarctica (Ross, 1991; Storey *et al.*, 1992; Omarini *et al.*, 1999; Cawood, 2005). The lithosphere in the study area was sufficiently strong (thick) for generating the extensional fracturing and buoyancy uplift. The continental dispersal from a triple-junction in Bolivia (Figure 1) produced, in NW Argentina, graben-like structures related to crustal thinning, topographic changes, and consequently gravity and geoid anomalies associated to the lithospheric extensional stress field, which may reflect an underlying structure that is implicit in the convective circulation of the mantle (Houseman, 1990).

Puncoviscana Basin's sedimentation initiated discordantly overlying the low-greenschist grade, banded metasandstones and metapelites of Medina Formation (López de Azarevich *et al.*, 2010b) (Figure 2a, Table 1). The sedimentary successions belong to Lerma Group (Salfity *et al.*, 1976) that registers a maximum thickness of 1,825 m (Omarini, 1983), with three characteristic sedimentation stages: i) Associated to marine and glaci-marine deposition, which includes the opening and the basal infilling of the basin; ii) Associated to postglacial chemical deposition distributed along the east margin; iii) Associated to tidal influenced episodes in a foreland basin that extended from final opening to closure of the basin, distributed all along and across the basin.

The first stage initiates with turbidites and diamictites of Sancha Formation (Ortíz, 1962). Van Staden and Zimmermann (2003) interpreted these basal diamictites in Corralito locality as lag conglomerate deposits, while the presence of glauconite points indicate an agitated, oxidized, shallow marine water.

During the second stage, cap carbonate sequences of Las Tienditas Formation and equivalent units of Volcán and Tumbaya formations (located northward) were deposited. The changing climatology and paleogeography contributed to biogeochemical and redox oscillations (Halverson *et al.*, 2009), and consequently to changes in the sedimentary facies and palaeoecological niches by the end of the Ediacaran that were able to establish a “carbonate factory” and consequently carbonate deposition in shallow platforms influenced by upwelling processes (López de Azarevich *et al.*, 2010b). Although there are no outcrops connected with carbonates from Tumbaya and Volcán formations located to the north, they record the same stratigraphic relation with transition to Puncoviscana Formation (Iturriza, 1981; López de Azarevich *et al.*, 2010b).

The third and last sedimentation stage corresponds to deposition of Puncoviscana Formation (Turner, 1960). The sequence displays shallow marine deposits influenced by tides, and few interlayered pyroclastic deposits. It has the configuration of a foreland basin (Ježek, 1990; Kraemer *et al.*, 1995; Keppie and Bahlburg, 1999; Zimmermann, 2005) and evolved from an initial arc-trench setting towards a syn-collisional foreland basin by 530 Ma (Escayola *et al.*, 2011). The paleontological record indicates that sedimentation occurred during the Ediacaran-Terraneuvian Series 2 stratigraphic interval with *Nemiana-Belltanelloides* (Vendian-Ediacaran) and *Oldhamia* (Early Cambrian) ichno associations (López de Azarevich *et al.*, 2012). These ages are consistent with those recorded by pyroclastic levels of 545-512 Ma (Escayola *et al.*, 2011; Aparicio González, 2014).

The source of the clastic material for Puncoviscana Formation (Ježek, 1990) points towards provenance from continental blocks and recycled orogens, supracrustal sedimentary orogenic belts and active-deformation belts. The geochemical signature of this lithostratigraphic unit suggests a provenance from continental to continental island arc settings, related to a magmatic source (Zimmermann, 2005; Escayola *et al.*, 2011; Piñán-Llamas and Escamilla-Casas, 2013). Zircons collected from the clastic sequences (Zimmermann, 2005; Aceñolaza *et al.*, 2010; Aparicio González *et al.*, 2010; Escayola *et al.*, 2011) yielded ages that indicate a dominant provenance from Archean and Palaeoproterozoic cratonic zones (2.7-2.0 Ga) southward, and Mesoproterozoic-Grenville rocks (1.5-1.0 Ga) to the northeast and west (Figure 1).

The closure of the Puncoviscana sea is coincident with the closure of others seas such as Iapetus Ocean southward. In NW Argentina, eastward compression produced the Pampean Orogeny (580-515 Ma, Sureda and Omarini, 1999). The emplacement of Tilcara Magmatic Arc (Tilcara Phase of Pampean Orogeny) is characterized by calc-alkaline plutons as early as 550 ± 26 Ma (Tipayoc Pluton, Omarini *et al.*, 1996), which is consistent with the oldest ages inferred from the fossil record. Final consolidation of Tilcara Arc is represented by the 520 Ma dykes intruding (Puncoviscana) Guachos Formation in Mojotoro range and the ~ 511 Ma Chañi Pluton.

Table 1. Stratigraphic correlation of the Neoproterozoic – Early Cambrian sedimentary units of Northwest Argentina.

	Location			
	NW Argentina	Lerma Valley	Sierra Mojotero	Isotopy / Zircon ages
Authors	Turner (1960)	Salfity <i>et al.</i> (1976)	Aparicio González (2014, and literature)	Sial <i>et al.</i> (2001), Toselli <i>et al.</i> (2005), López de Azarevich <i>et al.</i> (2010b) / Aparicio González (2014), Aparicio González <i>et al.</i> (2011)
First order stratigraphic unit	Puncoviscana Formation	Lerma Group	Puncoviscana Complex	
Second order stratigraphic units		Corralito Formation	–	
		Puncoviscana Formation	Guachos Formation	Zircons from 1.9-1.8 Ga, 1.2-0.9 Ga, 0.8-0.65 Ga and 0.55-0.52 Ga. Deposition at 540-520 Ma.
			Alto de la Sierra Formation	Zircon ages with dominant peak at 0.6-0.55 Ga. Deposition at 545-540 Ma.
	Volcán, Las Tienditas and Tumbaya carbonates	Volcán, Las Tienditas and Tumbaya Formations	–	
		Sancha Formation	Chachapoyas Formation	Zircon ages of 2.7-2.5 Ga, 2.2-1.8 Ga, 1.2-1.0 Ga and 0.7-0.6 Ga. Deposition at 570-545 Ma.

The deformation style of Puncoviscana Formation is associated to a progressively assembled accretionary complex during the Early Cambrian (Escayola *et al.*, 2011) and to flexure related to the sinistral NNW-SSE El Toro lineament during the Miocene (Hongn *et al.*, 2001).

CAP CARBONATES GEOCHEMISTRY

The cap carbonate sequences of Volcán, Tumbaya and Las Tienditas formations, deposited in a shallow-water platform overlying Sancha Formation (Figure 2a), crop out over a 50 km-wide belt along the eastern margin of the basin. Although Volcán Formation was considered the oldest carbonate deposit based on isotopic data (Sial *et al.*, 2001), the stratigraphic relation in León zone and the identified facies (Chiliguay *et al.*, 2019) contributed to understanding of a unique carbonate platform that includes all these deposits. The presence of equivalent carbonate platforms in South America evidence that, by time of deposition, basins around fragmented Rodinia were located near the Equator (Young, 2013) or at least in the 30°N to 30°S paleolatitude belt.

The analysis of major and trace element geochemistry of the carbonate facies (Table 2) provided significant insights about the palaeoenvironmental conditions during carbonate precipitation. As the Fe_T/Al ratio in carbonates would be enhanced in euxinic basins (Anderson and Raiswell, 2004; Lyons and Severmann, 2006), and can be used as an independent palaeoredox proxy, the Fe_T/Al ratio of 1.15 (average) characterizes a euxinic or anoxic sedimentation. In addition, the lack of iron sulphide (pyrite) suggests that Fe, as well as Mn, entered the crystalline structure of carbonates during deposition. Considering discussions in Huang *et al.* (2011) and Young (2013), the enrichment of redox-sensitive elements implies that the depositional environment in this carbonate platform was anoxic and ferruginous but not euxinic.

These paleoenvironmental conditions agree with the presence of carbonaceous substances in calcareous sequences of León-Volcán zone and rounded organic residues after treatment with HCl [50], while the chemical signature of cap carbonates is in concordance with results for the temporally equivalent carbonates of the basal section of Bambuí Group in Brazil (Kuchenbecker *et al.*, 2016).

On the other hand, the low Fe, Mn, Co, Y and V in the cap carbonates suggests that its genesis was not controlled by circulation of hydrothermal fluids along fractures associated to the rifting zone. Consequently, it implies that no oceanic hydrothermalism was active during the carbonates' precipitation, pointing towards a flexural foreland basin bounded by deformed orogenic belts (Pampia, Amazonia, and Antofalla) without generation of oceanic crust.

The isotopic variations of Sr, C and O in Las Tienditas Formation, analysed at a detailed scale (Table 3), record changes related to the sedimentary episode, and are a consequence of a delicate equilibria between the deposited facies and the sea water, the interchange with the atmosphere and the biosphere. The $\delta^{13}C$ values show a signature of +1 ‰ PBD distributed in most of the sequence with a negative excursion near the top of the profile (-2.16 ‰ PBD), interpreted as decrement on the biological productivity response (Sankaran, 2000), possibly related to anoxic water sourced to the basin. Changes of microbial mats development are evident from thin sections. Processes of rapid burial of photosynthesize organic matter and oxidation would enhance the changes in $^{12}C/^{13}C$ (Scholle and Arthur, 1980; Fike *et al.*, 2006). These values in the sequence are similar to that of the Cambrian carbonates of Sierra del Gigante, Caucete Group and La Laja Formation in Argentina (Sial *et al.*, 2001; Galindo *et al.*, 2004), and Corumbá Group in Brasil (Misi *et al.*, 2007).

Table 2. Geochemical analysis from Puncoviscana Basin' crystalline limestones, except sample 10 that is a diagenetic calcite vein. Data for Las Tienditas carbonates: 1 to 9 from Tapia Viedma and Gorustovich (1998), 10-11 from López et al. (2006), and samples* from Sial et al. (2001), ** subtotal. Data from Font et al. (2006) and Kuchenbecker et al. (2016) are included for comparison. Major elements in wt%, trace elements in ppm.

Sample	Reference	SiO ₂	Al ₂ O ₃	Fe ₂ O ₃	MnO	MgO	CaO	Na ₂ O	K ₂ O	P ₂ O ₅	TiO ₂	PPC	Total	Ba	Sr	Zr	Y	Co	V
1	Tapia Viedma and Gorustovich (1998)	1,94	0,59	0,23	0,04	0,42	52,57	0,15	0,05	0,11	0,004	42,51	97,87						
2	Tapia Viedma and Gorustovich (1998)	2,51	0,28	0,29	0,09	0,29	52,4	0,01	0,08	0,05	0,002	41,69	97,67						
3	Tapia Viedma and Gorustovich (1998)	2,91	0,63	0,26	0,1	0,24	51,91	0,01	0,09	0,05	0,005	41,57	97,77						
4	Tapia Viedma and Gorustovich (1998)	1,23	0,67	0,68	0,1	0,77	51,12	0,32	0,01	0,08	0,008	42,53	97,51						
5	Tapia Viedma and Gorustovich (1998)	2,31	0,59	0,49	0,09	0,43	51,83	0,07	0,1	0,07	0,005	41,9	97,87						
6	Tapia Viedma and Gorustovich (1998)	0,64	0,3	0,74	0,05	0,94	51,79	0,13	0,02	0,04	0,004	43,29	97,93						
7	Tapia Viedma and Gorustovich (1998)	0,53	0,22	0,26	0,06	0,52	53,87	0,11	0,01	0,07	0,004	43,1	98,74						
8	Tapia Viedma and Gorustovich (1998)	1,51	0,63	0,28	0,01	0,33	52,19	0,1	0,07	0,11	0,005	42,19	97,43						
9	Tapia Viedma and Gorustovich (1998)	1,69	0,49	0,4	0,07	0,49	52,21	0,11	0,05	0,07	0,005	42,35	97,85						
10	López et al. (2006)	1,61	0,21	0,06	0,01	0,68	54,92	0	0,01	0,09	0,01	41,5	99,09	17	1723	67	1	2	1
11	López et al. (2006)	6,03	1,07	0,13	0,01	0,94	50,41	0,11	0,52	0,08	0,01	40,25	99,56	13	687	27	nd	nd	8
1*	Sial et al. (2001)	1,92	0,17	0,1	0,01	0,16	55,2	0,11	0	0,18	0,01		57,86**		3062				
3*	Sial et al. (2001)	0,55	0,12	0,09	0,02	0,15	55,66	0,49	0	0,12	0,01		57,21**		3098				
5*	Sial et al. (2001)	1,15	0,1	0,06	0,02	0,11	55,85	0,1	0	0,09	0,01		57,49**		2538				
10*	Sial et al. (2001)	1,89	0,32	0,13	0,04	0,2	55,01	0,1	0	0,28	0,02		57,99**		1887				
12*	Sial et al. (2001)	9,84	0,43	0,18	0,04	0,36	49,17	0,08	0	0,02	0,02		60,14**		1336				
15*	Sial et al. (2001)	13,54	0,66	0,36	0,07	0,44	46,2	0,12	0,01	0,21	0,04		61,65**		940				
18*	Sial et al. (2001)	9,07	0,42	0,19	0,08	0,37	49,69	0,18	0	0,03	0,03		60,06**		369				
20*	Sial et al. (2001)	21,94	2,4	0,97	0,11	0,8	38,23	0,3	0,61	0,05	0,05		65,32**		536				
23*	Sial et al. (2001)	44,32	1,35	0,83	0,09	0,93	26,43	0,12	0,13	0,06	0,06		74,33**		229				
Ave.	Font et al. (2006)	0,62	0,27	0,45	0,18	20,54	31,6	b.l.m.	0,06	0,03	0,02	45,57	99,26						
Ave.	Kuchenbecker et al. (2016)	10,74	2,19	1,27	0,07	7,93	38,34	0,14	0,55	0,27	0,12	37,93	99,57						

Table 3. Fe, Mn and Al ratios for carbonates from Puncoviscana Basin' crystalline limestones, except sample 10 that is a diagenetic calcite vein. $\delta^{13}\text{C}$, $\delta^{18}\text{O}$ and $^{87}\text{Sr}/^{86}\text{Sr}$ are included. Data for Las Tienditas carbonates: 1 to 9 from Tapia Viedma and Gorustovich (1998), 10-11 from López *et al.* (2006), and samples* from Sial *et al.* (2001). Avg. 1 from Font *et al.* (2006), Avg. 2 from Kuchenbecker *et al.* (2016) and Avg. 3 from Huang *et al.* (2011) at Zhongling and Avg. 4 from Huang *et al.* (2011) at Longe are included for comparison.

Sample	Fe (%)	Mn (%)	Al (%)	Fe/Al	Mn/Al	Mn/Sr	$\delta^{13}\text{C}\text{‰}$	$\delta^{18}\text{O}\text{‰}$	$^{87}\text{Sr}/^{86}\text{Sr}$
1	0.0770	0.0031	0.0265	2.9061	0.1171				
2	0.0350	0.0015	0.0423	0.8256	0.0366				
3	0.0350	0.0039	0.0476	0.7339	0.0813				
4	0.0559	0.0062	0.0053	10.5678	1.1706				
5	0.0489	0.0039	0.0529	0.9247	0.0732				
6	0.0280	0.0031	0.0106	2.6419	0.2926				
7	0.0489	0.0031	0.0053	9.2468	0.5853				
8	0.0769	0.0039	0.0371	2.0758	0.1045				
9	0.0489	0.0039	0.0265	1.8494	0.1463				
10	0.0419	0.0077	0.1112	0.3774	0.0697	0.0450			
11	0.0909	0.0077	0.5664	0.1605	0.0137	0.1128			
1*	0.0699	0.0077	0.0900	0.7770	0.0861	0.0253	3.4	-6.9	0.70870
3*	0.0629	0.0155	0.0635	0.9907	0.2439	0.0500	2.9	-10.3	0.70875
5*	0.0419	0.0155	0.0529	0.7926	0.2926	0.0610	3.11	-8.8	0.70877
10*	0.0909	0.0310	0.1694	0.5366	0.1829	0.1642	1.23	-6.9	0.70878
12*	0.1259	0.0310	0.2276	0.5530	0.1361	0.2319	1.01	-6.86	0.70912
15*	0.2517	0.0542	0.3494	0.7205	0.1552	0.5768	0.19	-6.6	0.70928
18*	0.1328	0.0620	0.2223	0.5976	0.2787	1.6793	0.45	-6.6	0.70993
20*	0.6783	0.0852	1.2705	0.5339	0.0671	1.5897	-1.57	-5.55	0.70948
23*	0.5804	0.0697	0.7147	0.8122	0.0975	3.0443	-1.01	-6.44	0.710819
Avg.1	0.3147	0.1394	0.1429	2.2016	0.9755	0.0253			
Avg.2	0.8876	0.0521	1.15670	0.5735	0.0349	0.6731			
Avg.3	0.8	0.369		0.962	0.5190				
Avg.4	0.74	0.39		1.485	0.9175				

The $\delta^{18}\text{O}$ shows a progressive change from $\sim -8.00\text{‰}$ PDB at the base of the sequence up to three quarters (-5.27‰ PDB) and then an oscillation around -7.2‰ PDB. The signature is similar to other carbonates from NE Brazil (Sial *et al.*, 2000). In addition, the isotopic range of $^{87}\text{Sr}/^{86}\text{Sr}$ changes from 0.7080 to 0.71017 in the same section and stabilizes around 0.7080. This pattern is similar to other post-glacial carbonates deposited during post-Gaskier episodes. High $^{87}\text{Sr}/^{86}\text{Sr}$ values would be consequence of erosion/weathering processes in the sourcing areas that favoured the enrichment of radiogenic, continental derived ^{87}Sr (Melezhik *et al.*, 2001) in decrement of marine ^{86}Sr .

PUNCOVISCANA FORMATION

Above the cap carbonate sequence the sedimentation changed and progressively incorporated fine clastic shallow marine deposits, evidenced by interlayering of siltstones of Puncoviscana Formation (Iturriza, 1981; López de Azarevich *et al.*, 2010b), as recognized along the eastern margin of the basin (Figure 2). Along the western margin and in the area of sierra de Mojotoro, it shows a tectonic contact with the clastic successions of Sancha Formation (Table 1).

When these units outcrop close to granitic intrusions (e.g., Tastil), Sancha Formation develops biotite recrystallization due to thermal metamorphism driven by the granitic intrusion (~550-533 Ma), whereas Puncoviscana Formation outcrops are juxtaposed by fault contact showing very low metamorphic grade with an anchizone mineral assemblage.

The structural signature of the Neoproterozoic – Early Cambrian sedimentites is of a north trending, east-vergent, folded and faulted belt. Within this belt, stratification and folding of Puncoviscana Formation changes depending on regional structures defined within Choromoro and Lules-Puncoviscana belts (see discussions in Mon and Hongn, 1991, 1996), located west and east of the central axis of Puncoviscana Basin, respectively. The western Choromoro Belt conforms an antiform that exhibits three deformational events, a higher deformation grade and east-vergent chevron-like structures. It over-thrusts the eastern Lules-Puncoviscana Belt, which exhibits two deformational events, lower deformational grade and WNW-vergent asymmetric folding. Hence, the basin axis is represented by a major tectonic structure within Proterozoic terrane assemblage (i.e., a previous suture zone, Figure 2c).

Puncoviscana Formation is composed of grey to greenish (occasionally reddish) marine mudstones and fine sandstones, with scarce conglomerates that develop channel architectures. It is characterized by lithologic homogeneity, shallow water sedimentary structures, trace fossils and soft body impressions that evidence coastline palaeoenvironmental conditions with tidal flooding and wave action (López de Azarevich *et al.*, 2010e, 2012).

Five sedimentary sections (SP) of Puncoviscana Formation were analysed along the East (1) and West (4) margins of the basin (Figure 3). The sections conform up to 100 m-thick, undisturbed sequences that record a faulted or covered base. At the top, they exhibit a discordance with Palaeozoic or modern sedimentary units. Sequences are grey to greenish, have geochronological and biostratigraphical control, and do not record structural discontinuities.

The depositional time span is consistent with the ichnofaunas associations identified by Aceñolaza and Aceñolaza (2005), Buatois and Mángano (2012), and Chiliguay *et al.* (2014, 2016) consisting of *Helmintoidichnites* and *Helminthopsis* (lower Ediacara, 560-550 Ma), *Treptichnus* (upper Ediacara, 550-542 Ma) and *Oldhamia* and *Hydrozoa* (Early Cambrian). The upper limit is bounded by ages of interlayered volcanites and intrusions of late plutons and dykes (523-511 Ma). Radiogenic ages obtained from primary magmatic zircons span from 545 Ma (Purmamarca SP, East Margin) and 523 Ma (Rancagua SP, West Margin), according to data in Aceñolaza *et al.* (2010) and Adams *et al.* (2008), respectively. Depositional ages of the interlayered pyroclastic rocks, volcanoclastic grains contained in the sandstones facies and geochemical signatures of clastic sequences set the sedimentation during the active margin stage once the magmatic arc started to develop (Escayola *et al.*, 2011, and literature).

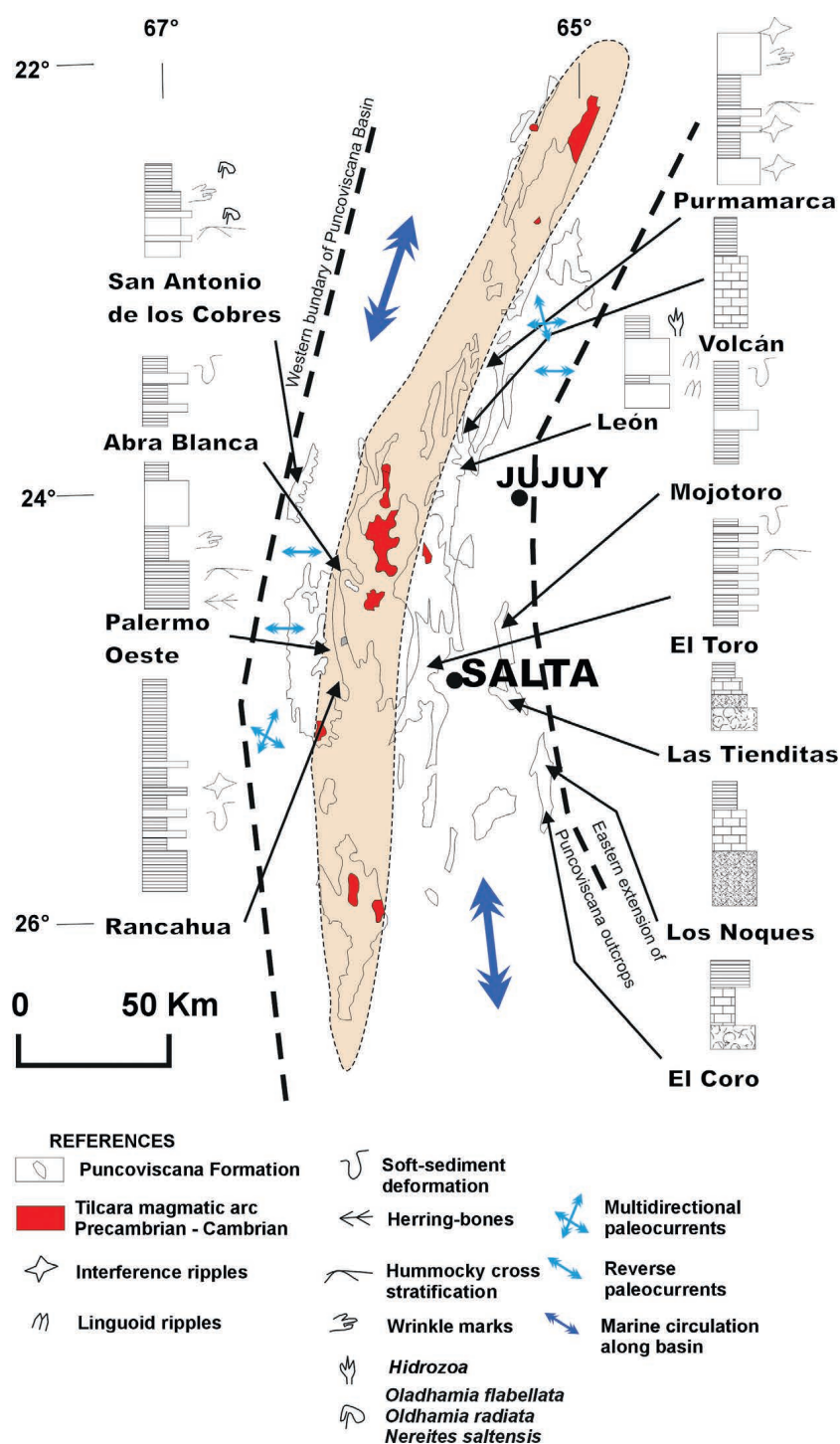


Figure 3. Integration of 12 lithostratigraphic sections and their distribution along and across the Puncoviscana Basin outcrops. Only along the Eastern Margin the stratigraphic sequence includes diamictite and cap carbonates facies, underlying the Puncoviscana Formation. Diagnostic sedimentary or biological structures are indicated along both margins.

The facies analyses were carried out in the clastic sequences of Puncoviscana Formation. Lithofacies were described in terms of dimension, morphology, and hydraulic features to explore the sedimentological processes, and are presented below and summarized in Table 4.

Table 4. Lithofacies associations in Puncoviscana Formation profiles.

Lithofacies	Denomination	Hydrodynamics	Reference
HCS	Hummocky cross-stratified sandstones	Combined action of unidirectional turbulent and oscillatory flows below the fair-weather wave base.	Harms <i>et al.</i> (1975, 1982), Bourgeois (1980), Dott and Bourgeois (1982), Walker and Plint (1992)
Sm	Massive sandstones	Progressive aggradations from nearly stationary flows, associated to bioturbation.	Nichols (2009)
Sl	Laminated sandstones	Progressive aggradation from nearly stationary background flows, associated to subtratal erosion. Bedload transport under an intermediate to high velocity flow regime, assumed 0.8 to 1.2 m/s.	Hjulstrom (1935), Allen (1968), Press and Siever (1986), Ginsberg <i>et al.</i> (2009).
Src	Current rippled sandstones	Traction-sedimentation from dilute fluxes, 2D and 3D ripples migration, bidirectional reverse paleocurrents, asymmetrical velocities for flood and ebb tides with reworked, secondary ebb-oriented crests. Combination of ebb-flood currents and littoral drift. Water depths of several meters or less.	Allen (1984), Davis and Dalrymple (2012), Archer (2013)
Srw	Wave rippled cross lamination	Oscillatory fluxes related to wave's dynamics. The flux energy was high enough to produce rounded symmetric crests due to vortex development near the bottom surface.	Nichols (2009)
Ch	Channel forms	Produced by two stages: 1) Generation of the basal erosional surface during ebb tides, while scour characteristics and channel dimensions suggest a moderate-energy flow; 2) Deposition of reworked material from the older platform sequences (either clastic or carbonate) accompanied by sandy and/or silty matrix. Transport developed with a flow velocity of ~3.50-1.10 m/s and deposition occurred once it decreased to <0.5 m/s.	Hjulstrom (1935), Press and Siever (1986)
Ht	Heterolithic	Ht facies formed by bimodal (mud/sand) bipolar currents produced by two energy flows: bedload transport by tidal currents that generated the sandy ripples, and settling from suspension during periods of standing water (high or low stand) of the silty material.	Pettijohn and Potter (1964), Pettijohn (1975)
Htc	Heterolithic convolute stratification	Interpreted as hydroplastic efforts due to trapped air in intertidal plains. Deformation occur when flood progress before air could scape from the pores.	de Boer (1979)
Mmd	Desiccation structure, massive mudstone	Periodic episodes of sub-aerial exposure in intertidal zones, sometimes enhanced by microbial activity.	Nofke (2010)
MI	Laminated mudstones	Low wave action, currents associated to tide action, important biological activity and runoff in intertidal zones. High-rate source of fine material by continental drainage, which was reworked and deposited by tides.	Bryce <i>et al.</i> (1998)
MLrh	Laminated rhythmites	Alternating flood and ebb tidal currents in intertidal to subtidal environments. They reflect cyclical variation in the current competence and accumulation capacity. The cyclicity of these deposits indicates a diurnal tidal regime and synodic and tropical periods were recognized.	Williams (1991), Mazumder and Arima (2005), López de Azarevich (2010), López de Azarevich <i>et al.</i> (2010a-d), Longhitano <i>et al.</i> (2012), López de Azarevich and Azarevich (2015a, 2017)

Rancagua sedimentary profile

The section is located on Route N° 40, nearby the town of Rancagua. It represents an icely preserved undeformed section of Puncoviscana Formation, 87.5 m-thick oriented 212°/50° (DD/D). The base is covered and at the top of the sequence a fault is juxtapose undifferentiated metasedimentites. The sedimentary profile comprises a fining upwards sequence in which three sections are identified: i) lower, ii) medium, iii) upper, with the following facies associations (Figure 4 and 5):

Lower section: Shoreface Lithofacies Association.— The lower section of the profile is 52.5 m thick, in which facies Sl, Sm, HCS, Src and Swr are recognized. The ratio of coarse sandstone relative to medium-fine sandstone is 3/1 (Figure 4a).

The section begins with 10 m of medium to coarse sandstones, with thick planar tabular stratification of 7-14 cm (facies Sl). These are stratified in 40 cm-thick banks with net surfaces that are planar at the base and undulating on top. Interbedded are 15-45 cm-thick fine sandstone banks, with flat or oblique small-scale planar stratification and occasionally trough stratification (facies Scr).

Sedimentation continues with 25 m of fine sandstones developing facies Scr with tangential cross-bedding (single and double), and oblique flat tabular stratification, accompanied by interbedded medium sandstones with flat erosive surfaces at the base and undulating on top. Interference and linguoid ripples are also recognized in several levels. Flute casts are also common, whose dip dimensions are enhanced by impacts driven by mud flakes.

The last 17.5 m of this section is characterized by fine to medium sandstones with facies Swr and tangential single stratification, and also flat tabular cross and trough stratification, and interference ripples towards the top (facies Scr). Straight ridges ripple marks are found in successive banks that addresses changes of 40° in flow direction. There are also groove and punching casts produced during the runoff.

Palaeocurrents in this lower section changes according to hydrodynamics of the process producing the sedimentary structures. Unidirectional structures such as flute casts generated during ebb indicate NNW- and NE-directed currents. Current ripples indicate unidirectional palaeocurrents in different trends: towards N and NNW as well as W-E. Finally, interference ripples register NNW-SSE directions and resemble oblique flux due to longshore currents along the coastal setting.

Middle section: Nearshore Lithofacies Association.— The middle section of the profile is 22.5 m thick, in which facies Sl, Ml, Htc, HCS and Src are recognized. The ratio of sandstone relative to mudstone is 3/1 (Figure 4b).

This section comprises a regular interlayering of medium sandstones and mudstones along the stratigraphic high. Sandstones develop cross-bedding, fine sandstones with parallel lamination or undulating, and trough stratification and symmetrical and asymmetrical ripple marks on top, stratified in 15 cm-thick banks. Mudstones develop regular lamination within 10-15 cm-thick banks, occasionally developing cross-bedding and mimic the structure of the base line ripple marks. They occasionally develop Ht facies with convolute stratification and undulitic to lenticular stratification. Microhummocks, mud flakes, gutter casts and saltation marks evidence higher energy flux possibly related to storm episodes.

Palaeocurrents measured from unidirectional sedimentary structures are oriented towards NE and WNW. Ichnogenus *Helminthoraphe* and *Trepichmus* are present.

Upper section: Offshore Lithofacies Association.— The upper section of the profile is 12.5 m thick, in which facies Sl, Ml, HCS and Src are recognized. The ratio of sandstone relative to mudstone is 1/10 (Figure 4c).

This section comprises 12 m of rhythmic laminated mudstones (Mlrh) stratified on decimeter scale with mm-thick internal lamination, interbedded with 3 cm-thick fine to medium sandstones, massive or developing trough stratification that show erosive bases and symmetrical ripple marks on top. The inner lamination thickness resembles a graded sequence in which sandstones are clearly subordinate.

Palaeoenvironmental evolution.— The lower section is characterized by shoreface facies associations. Facies pass from asymmetrical to symmetrical ripples, indicating a systematic change of orbital intermediate to unidirectional flows, respectively. Likewise, the combination of flat layers, troughs and ripple marks indicate orbital intermediate unidirectional flows that allows the migration of 2D and 3D wavelets. Multidirectional palaeocurrents suggest changes in wave trend and possibly combined flows. The hydrodynamics of the environment is characterized by the interaction of N-directed currents representing the ebb tidal flux parallel to the N-S trending of the basin and multidirectional palaeocurrents as a consequence of wave trend and littoral drift interaction. The sets of planar layers of high flow regime associated with sets of cross stratification, and groove and puncture casts produced during ebb, indicate shoreface to foreshore environments.

The middle section indicates a nearshore environment, governed by periods of low energy deposits by decantation and high energy periods dominated by tidal currents and storm events in a proximal shelf environment. Multidirectional palaeocurrents are preferentially northward and indicate that palaeoflux followed the basin elongation.

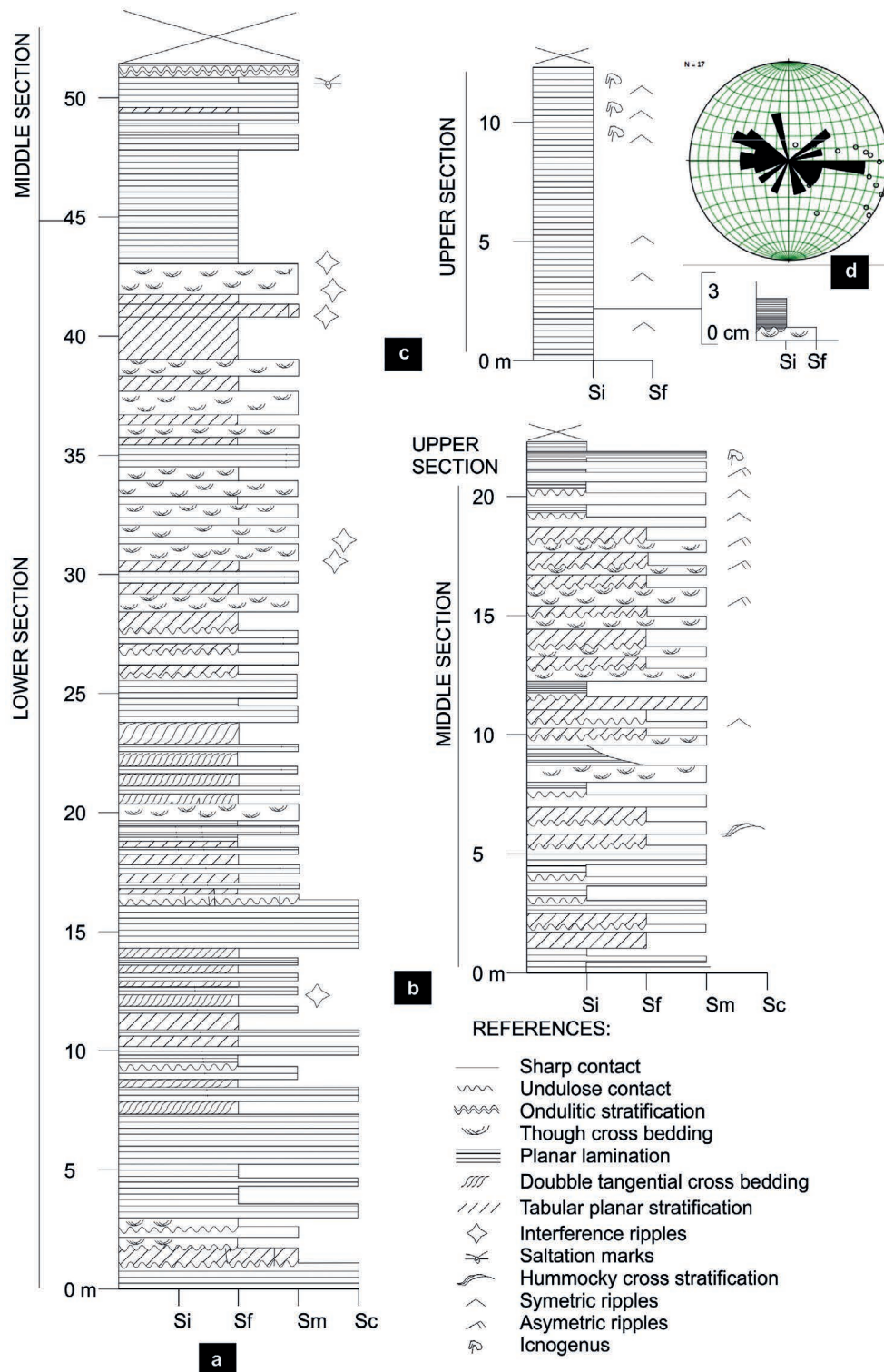


Figure 4. Sedimentary section of Rancagua SP. a. Lower section. b. Middle section. c. Upper section. d. Palaeocurrent diagram.

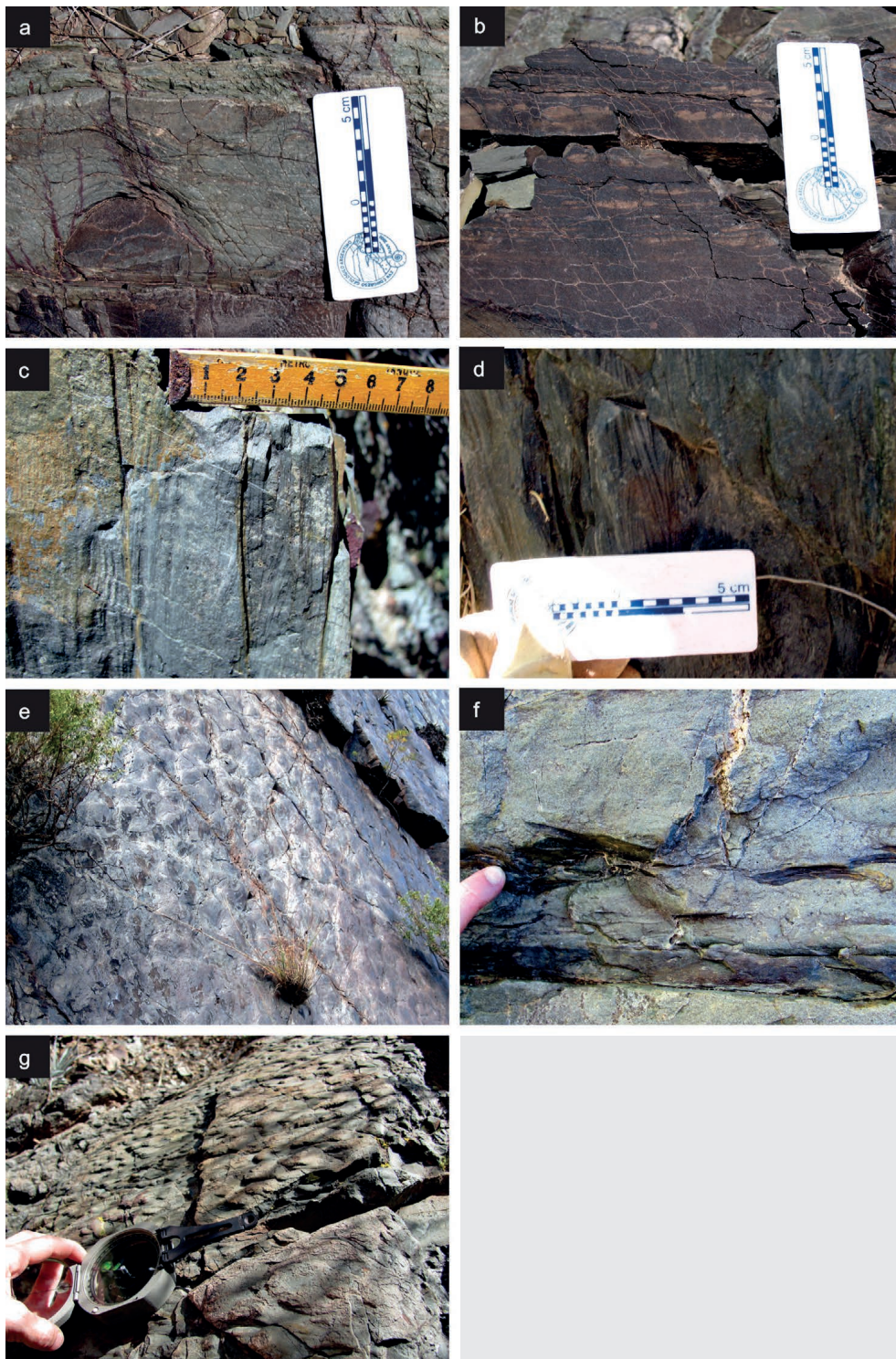


Figure 5. Sedimentary structures at Rancagua SP. a. Convolute stratification (facies Htc). b. Lenticular stratification in Ht facies. c. HCS facies. d. Wavy ripple lamination (Srw facies). e. Interference ripples (facies Src). f. Mud flakes. g. Linguoid ripples (facies Src).

The upper section resembles atide-dominated shelf as evidenced by the association of basal ripple sandstones passing to heterolithic facies with sandy lenses and increased clay proportion. The rhythmic graded successions of sandy-silty banks fining upwards with abundant trace fossils and few interbedded storm levels, and hummocky and trough stratification imply atidal flat environment in subtidal and transitional to distal platform (nearshore to offshore). This environment, protected from wave action, allowed the preservation of the tidal rhythmic sequence. The fine sediments that entered the movement during the ebb tides are transported mainly in suspension along ebb tidal channels towards the offshore. There, suspended sediments are deposited in finely laminated, fining upward graded series. These graded rhythmites of tidal origin are similar to those of Reynella siltstone, of the Upper Neoproterozoic from South Australia (Williams, 2000).

Analysis of lithofacies associations in Rancagua SP involves a deepening sequence from a wave and tide-dominated intertidal shoreface, which evolves towards subtidal nearshore environments with predominance of tidal processes and storm episodes, and finally to subtidal environments below the storm level in a tide-dominated offshore (López de Azarevich *et al.*, 2010a).

These associations reflect a pericontinental shallow shelf environment (<200 m-deep) with a shoreline-shelf profile that records a period of aggradations with good sediment supply (Johnson and Baldwin, 1996) and abundant organic activity.

Considering statements presented by Selley (1968) regarding the three parameters that define a palaeocurrents model, the multidirectional palaeocurrents in the Rancagua SP evidence the following signatures:

- Environment (depositional process): Shallow marine environment characterized by tidal currents and littoral drift, with transgressive profile.
- Azimuthal paleocurrent pattern at outcrop: Polymodal paleocurrent patterns driven by tractive processes alongshore, offshore and onshore (Figure 4d). It shows bimodal bipolar (herringbones) and bimodal transversal data (interference ripples).
- Relationship between paleocurrents and paleoslope: Although a northward dipping paleoslope is deduced due to basin configuration and seawater outflow, this parameter cannot be defined adequately.

Palermo Oeste sedimentary profile

The profile is located in the outskirts of the town of Palermo Oeste. It represents an undeformed section of Puncoviscana Formation, 63 m-thick, with excellent presentation and preservation, oriented 290°/77° (DD/D). The base is covered, and at the top of the sequence a fault is juxtaposed to undifferentiated metasedimentites. The lithofacies associations allow recognition of three sections (Figure 6):

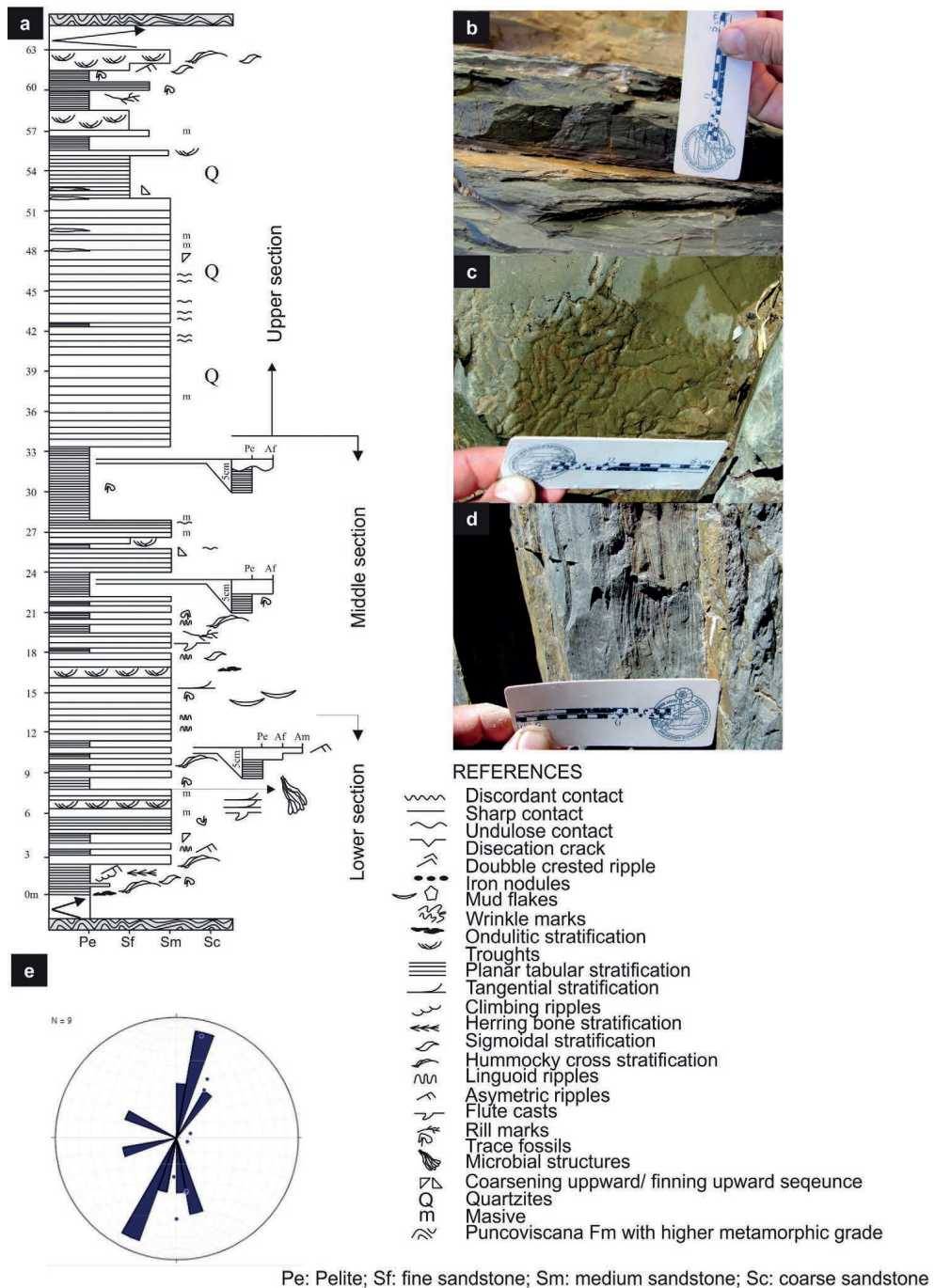


Figure 6. a. Sedimentary section at Palermo Oeste SP. b. Herring bones. c. Microbial mats. d. Facies Src, troughs. e. Palaeocurrents diagram.

Lower section: Intertidal Lithofacies Association.— The lower section is 33 m thick and registers an interlayering of medium sandstones and mudstones with an abundant trace fossils association equivalent to Rancagua SP, microbial mats and subaerial exposition evidence. The sandstone/mudstone ratio is 1/1.

The section begins with 8 m of small-scale (5 cm) cross-stratified sandstones (facies Scr) interlayered with laminated mudstones (facies Ml) and a heterolithic facies (Ht) with lenticular lamination. Facies Scr includes tangential cross bedding, linguoid ripples and troughs. Small wrinkle marks and flute casts are also common. At 7 m of the stratigraphic column, a huge microbial structure is registered all along the strata surface, accompanied by elephant-skin marks.

The following 3 m are represented by laminated rhythmic, inverse grading mudstone to medium sandstone banks that develop cross bedding and eventually HCS facies.

This is followed by 16 m of sandstones with linguoid ripples, though cross bedding, tangential stratification (facies Scr) and HCS facies. Mudstones are interlayered in inverse grading successions, as mud flakes included within sandstones and laminated levels (facies Ml and Ml_{rh}) that include trace fossils and rill marks. The last 6 m is composed only by facies Ml_{rh} with trace fossils.

Palaeocurrents measured from unidirectional sedimentary structures are towards W, NE and NW, and less commonly towards SE and SW. Wrinkle marks are oriented preferentially westwards and display a gentle dip above the whole sedimentary plane. The palaeontological association includes *Cochlichnus*, *Treptichnus*, *Glokeria*, *Helminthopsis*, *Helmintoraphe*, *Nereites*, *Oldhamia radiata* and *Oldhamia flabellata*.

Middle section: Shoreface Lithofacies Association.— The middle section is 23 m thick and is characterized by a homogeneous sandstone composition, and scarce mudstone lenses. It begins with 19 m of massive sandstones and quartzites stratified in up to 1 m-thick layers, sometimes developing internal lamination (facies Sm and Sl), separated by few levels and lenses up to 20 cm-thick of laminated mudstone (facies Ml). Upwards, it follows with 3 m of fine sandstones, laminated in 5-15 cm-thick banks (facies Sl and Ml).

Upper section: Intertidal Lithofacies Association.— The upper section of the profile is 8 m thick, in which facies Sl, Sm, HCS, Src and occasionally Ml are recognized. The ratio of medium sandstone relative to mudstone is 5/1. It registers an interlayering of cross-stratified medium sandstone (facies Scr) with laminated mudstones (facies Ml), with few levels of medium sandstones with hummocky cross stratification (facies HCS). These are stratified in 10 to 50 cm-thick banks. Facies Scr is characterized by double tangential and tabular planar cross stratification, climbing ripples

and herring bones. Mudstones show rill marks, abundant trace fossils, and develop an undulose contact at the top.

Palaeoenvironment evolution.— The basal section indicates a tide-dominated shelf as evidenced by the association of heterolithic facies with rill marks, microbial activity and flute casts associated to ebb currents. The rhythmic graded successions of sandy-silty banks with abundant trace fossils and few interbedded levels with hummocky HCS imply an intertidal environment of a tidal flat. Palaeoflux directions evidence that ebb tidal currents dominated the environment dynamics.

The middle section is characterized by regular facies of homogeneous sandstones arranged into sets of planar layers of high flow regime alternating with massive banks that evidence accretion in a shoreface environment.

The upper section shows domination by waves and tides. The conjunction of Scr facies with HCS and climbing ripples evidence wave action and different flux velocities associated to sand transport, while Ml with rill marks and abundant organic activity, together with herring bones, evidence tidal action along the intertidal zone.

Analysis of lithofacies associations in Palermo Oeste SP involves a tidal flat sedimentary system that evolves from intertidal to shoreface and to intertidal again, in which the biogenic activity has played an important role throughout the entire period of recorded sedimentation. On this tidal flat, bottom shapes are represented by diverse ripple marks, whose development was controlled by the water depth, the bottom shear and the grain size (Middleton and Southard, 1984). These morphologies were developed mainly during the ebb tide, along intertidal to subtidal environments, as have been found in other tidal plains (Vos and Erikson, 1977; Eriksson *et al.*, 1998; Chakrabarti, 2005; Guidi *et al.*, 2005). Palaeoflux directions evidence ebb tidal currents as dominating the environment dynamics.

Considering statements presented by Selley (1968) regarding the three parameters that define a palaeocurrents model, the multidirectional palaeocurrents in the Palermo Oeste SP evidence the following signatures:

- Environment (depositional process): Shallow marine environment characterized by tidal currents on the photic zone and intertidal environments.
- Azimuthal paleocurrent pattern at outcrop: Polymodal paleocurrent patterns driven by tractive processes mostly alongshore that display bimodal bipolar data (herringbones) (Figure 6e).
- Relationship between paleocurrents and paleoslope: A NNE-ward dipping paleoslope is deduced due to basin configuration and seawater flow and outflow alongshore.

The conjunction of the following sedimentary structures are characteristic of this tidal plain: small-scale cross stratified lamination, cross-wavelet mega and trough stratification (2.5 to 5 cm) in sandy layers, out of phase ripple marks (climbing ripples), hummocky cross stratification, graded rhythmites of tidal origin, mud flakes associated with wave ripple marks, undulitic stratification and herring bone. These sedimentary structures are similar to those described by Ehlers and Chan (1999), Chakrabarti (2005), and literature therein.

The horizontal parallel stratification with uniform or non-uniform lamination and structures formed by unidirectional currents in the sandy layers (Src, Sl) characterize a process of beach accretion with predominance of wave action. These types of well-sorted and homogeneous sand deposits, with a high degree of maturity, are equivalent to those of actual beach faces (Walker and Plint, 1992).

Abra Blanca sedimentary profile

The profile is located on Route No. 40 near Abra Blanca town. It represents an undeformed section of Puncoviscana Formation, 28 m-thick, with excellent presentation and preservation, oriented $253^{\circ}/76^{\circ}$ (DD/D). The base and the top are covered. The sedimentary profile comprises a fine-medium grained sequence in which three sections are identified, belonging to intertidal and subtidal lithofacies associations (Figure 7).

Lower section: Intertidal Lithofacies Association.— The lower section of the profile is 9 m thick, in which facies Ml, HCS, Htc and Src are recognized. The ratio of medium sandstone relative to mudstone is 1/2.

It registers a regular heterolithic sequence of interlayering rippled sandstones and laminated mudstones. Sandstones are 4-5 cm-thick and develop a net base and undulating top, sometimes with internal Scr and HCS. Basal bioturbation is also common with horizontal and vertical domichnias forms. Centimetre-scale load casts of Htc facies in some banks could be indication of hydroplastic efforts due to trapped air in intertidal plains. Deformation occurs when flood progresses before air can escape from the pores. Mudstones are stratified in 5 cm average banks, internally laminated, widely bioturbated.

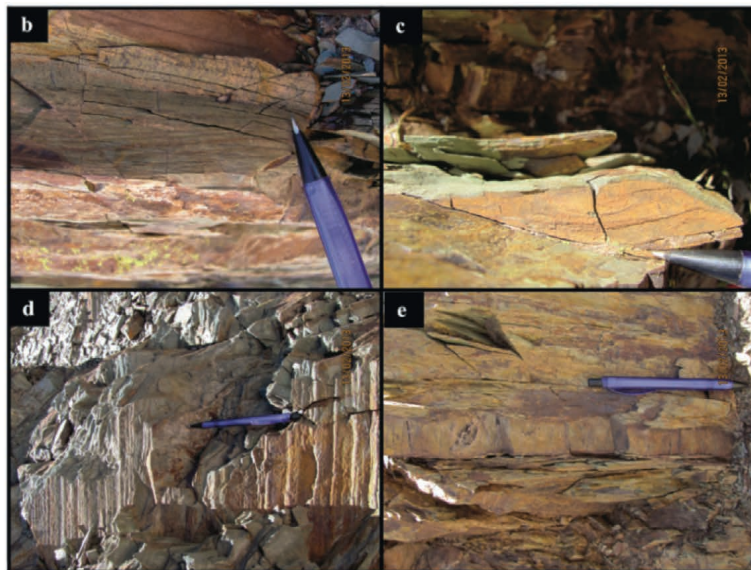
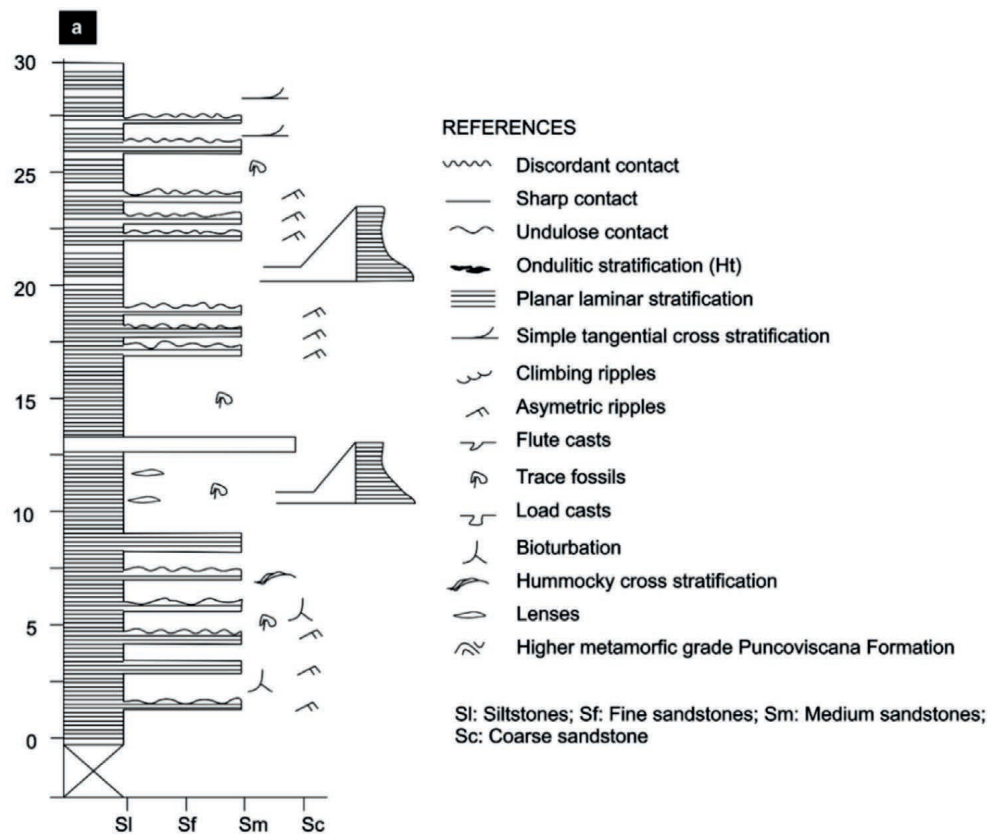


Figure 7. a. Sedimentary section at Abra Blanca SP. b. Facies Scr with planar stratification. c. Facies Scr with tangential stratification. d. Tidal rhythmic sequence (facies Mlrh). e. Ripple surface filled up with laminated siltstone.

Middle section: Subtidal Lithofacies Association.— The middle section of the profile is 8.5 m thick, in which facies Ml_{rh} and occasionally Sm and only one level of Ch are recognized. The ratio of medium sandstone relative to mudstone is 1/50. It is characterized by extremely regular rhythmic successions of internally laminated 10 cm-thick muddy banks. Scarce sandstone levels and lenses less than 5 cm-thick are found, as well as one level of basal coarse sand. Bioturbation is widely distributed throughout the mudstone layers. The facies Ch is composed of a clastic pebble conglomerate level, 5 cm-thick level, with decens of cm lateral continuity.

Upper section: Intertidal to Subtidal Lithofacies Association.— The upper section of the profile is 10.5 m thick, in which facies Ml, Scr, HCS and occasionally Sm are recognized. The sandstone/mudstone ratio is 1/7. It registers a regular sequence of interlayered rippled sandstones and laminated siltstones. Sandstones are 4-5 cm-thick and develop a net base and undulating top, sometimes with internal Scr (planar and tangential) and HCS, or filled with laminated mudstones. Mudstones are stratified in 5 cm average banks, internally laminated, widely bioturbated with horizontal traces. The regular successions resemble tidal rhythmites, interlayered with few storm episodes possible due to seasonality.

Palaeoenvironmental evolution.— The basal section is dominated by tides in intertidal settings, regularly affected by wave action (Scr with HCS facies). Facies Ml associated with hydroplastic syn-sedimentary deformation together with abundant organic activity, evidence tide action along the intertidal zone.

The middle section registers a subtidal setting within a tidal flat environment, in which the very fine sediments as source material dominates. Small and scarce tidal channels were filled by coarse material evidencing erosion in the source areas.

The upper section environment is dominated by tides and affected regularly by wave action (Scr with HCS facies). Facies Ml associated with abundant organic activity and tidal rhythmites evidence tide action along the intertidal to subtidal zone.

Atide-dominated shelf is evidenced by the association of Ml facies with tidal rhythmites, microbial activity and conglomerates suggesting channels developed by ebb currents. The rhythmic graded successions with abundant trace fossils and few interbedded levels with hummocky HCS imply an intertidal environment of a tidal flat.

Lower section: Subtidal Lithofacies Association.— The lower section of the profile is 8 m thick, in which facies Ml, Mlrh, HCS and Src are recognized. The ratio of medium sandstone relative to mudstone is 1/10.

It registers laminated mudstones stratified in 5-10 cm-thick banks, with *Nereites* and *Oldhamia* ichnoassociations. Undulating to lenticular and swaley stratification are common in the bottom, whereas tidal rhythmic lamination is identified towards the top. Impact marks of prod-type suggest saltation of gravel or coarse sandstone in the surface bottom. Interbedded sandstone lenses and coarsening-upwards levels with HCS and ripple marks at the top indicate discrete but periodic wave and storm action.

Middle section: Nearshore Lithofacies Associations.— The middle section of the profile is 3.5 m thick, in which facies Sl and HCS are recognized. The ratio of medium sandstone relative to mudstone is 10/1. It consist of regular sandstone banks, 10 cm-thick, developing facies HCS at the base and lamination at the top.

Upper section: Subtidal Lithofacies Association.— The upper section of the profile is 7.5 m thick, in which facies Ml, Mlrh, Ht, Scr and Sm are recognized. The ratio of medium sandstone relative to mudstone is 1/10.

It begins with laminated mudstones (facies Ml) stratified in 5-10 cm-thick banks, with *Oldhamia* ichnoassociations. Lenticular stratification (facies Ht) is common in the base and lamination at the top, whereas rhythmic lamination (facies Mlrh), of possibly tidal origin is identified throughout the section. Basal pebbles aligned with current ripples (facies Scr) are followed by laminated mudstone beds with abundant bioturbation that includes *Oldhamia flabellata*. This identifies erosion of the substrate and higher energy flow possibly during ebb. Very scarce sandstone lenses and levels are interlayered in the sequence.

Palaeoenvironment evolution.— The basal section resembles a tidal flat setting belonging to a tide-dominated shelf, characterized by a fine sediment source, abundant bioturbation and few storm episodes.

The middle section lithofacies associations suggest a wave-dominated setting that would include storm episodes in the nearshore, between the fair weather and the storm wave base, possibly resembling seasonal variations affecting a shallow shelf.

The upper section registers a subtidal, tide-dominated shelf (tidal flat) with abundant bioturbation during fair weather.

This profile registers a tidal flat environment in which a higher energy episode is intercalated, with a change in material sourced to the platform (sands dominating over mud) and wave action. This shift between tidal flat to nearshore associations with some storm episodes could be evidence of seasonal periods.

Purmamarca sedimentary profile

The profile is located on Route No. 9 arriving at the town of Purmamarca. It represents an undeformed section of the Puncoviscana Formation, 72 m-thick, with excellent presentation and preservation, oriented $296^{\circ}/76^{\circ}$. The lower and upper contacts are faults that in the base place the measured profile above undifferentiated levels of Puncoviscana Formation, and at the top fault is in contact with sedimentary sequences of the Ordovician Santa Victoria Group. The depositional sequence identifies three sections: i) lower, ii) medium, iii) upper, with the following facies associations (Figure 9):

Lower section: Nearshore Lithofacies Association.— The lower section of the profile is 12 m thick, in which facies HCS, Sl, Sm and Src are recognized. The ratio of fine sandstone relative to mudstone is 5/1. The first 10 m are a sandy-muddy sequence containing well-selected fine sandstones, stratified in thin banks internally massive or laminated, separated by flat surface sand scarce silty banks or mud flakes (facies Sl and Sm). In the lower section a first episode records sub-rounded structures produced by subaerial exposure (facies Sm) with desiccation and sub-rounded structures, while in the upper section there is an increase in laminated mudstones interbedded with sandstone facies. Upwards, there is interlayering of small-scale ripples, trough structures and hummockies formed by unidirectional currents related to tidal flows (facies Src) and storm waves (facies HCS). The presence of mud flakes and small channels indicate erosion processes and possibly channeling of the flow during ebb.

Middle section: Offshore Lithofacies Association.— The middle section of the profile is 10 m thick, in which facies Ml, Mlrh and scarce Sm or Scr are recognized. The ratio of fine sandstone relative to mudstone is 1/10. It consists of laminated mudstones interlayered with scarce fine sandstones, both with positive gradation, which belong to rhythmic tidal registers. Current ripples (facies Scr) develop planar and tangential cross bedding, suggesting few higher energy episodes linked to wave action during storms.

Upper section: Nearshore Lithofacies Association.— The upper section of the profile is 50 m thick, in which facies HCS, Sl, Sm, Src, Ml, occasionally Ch are recognized. The ratio of sandstone relative to mudstone is 1/1. It begins with 15 m of fine sandstone in facies Src, Ch and Sm with wavelet surfaces, and one level with desiccation cracks that represents subaerial exposure (in facies Sm). The next 12 m correspond to facies HCS and Scr that includes linguoid ripples and numerous wavelet surfaces. Wrinkle marks are common. It culminates with 1.5 m of red mudstones, with punctuation marks and soft body impressions, suggesting high speed turbulent flow levels with good biological productivity in shallow water, and oxidizing events within the intertidal zone.

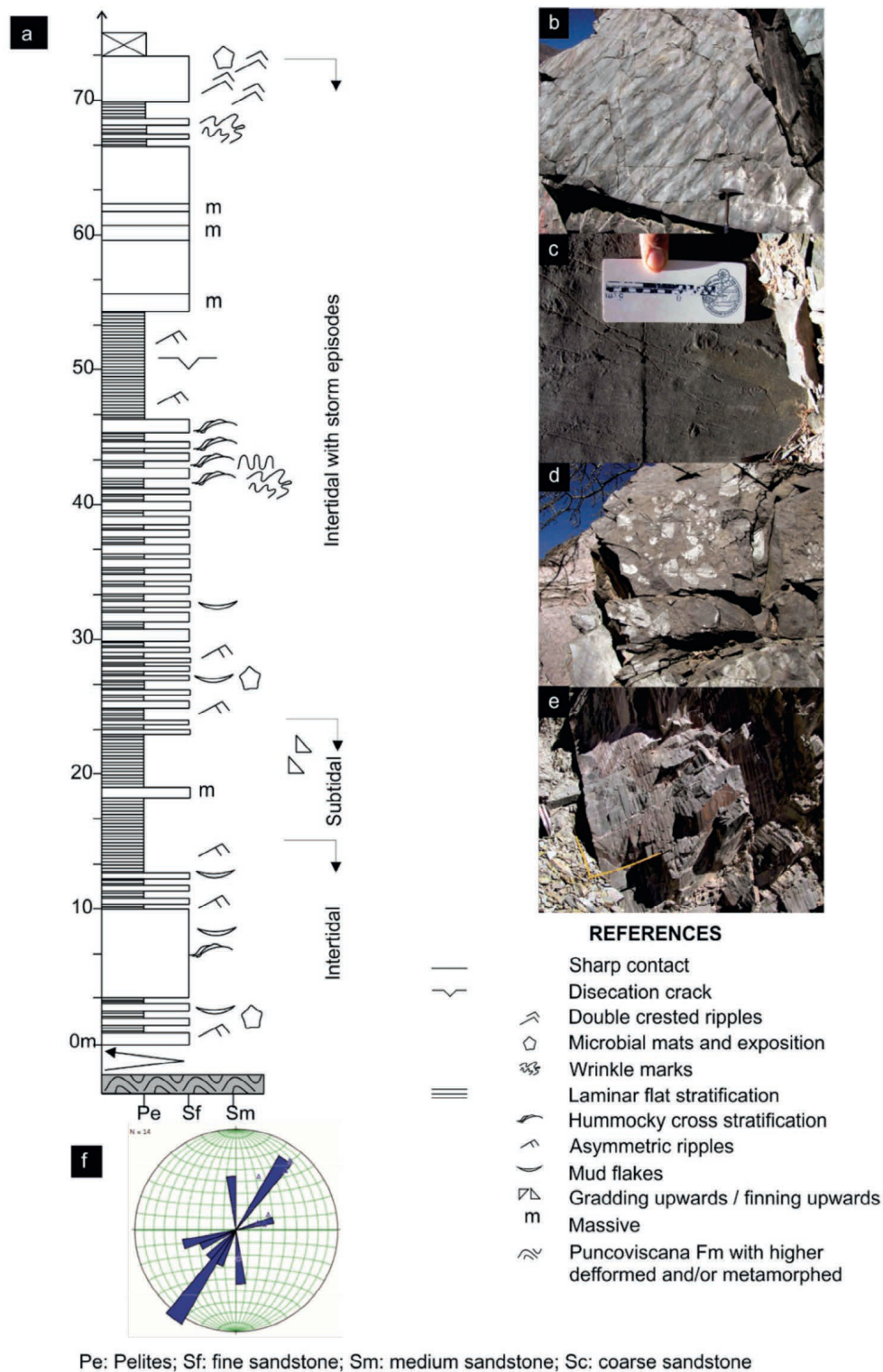


Figure 9. a. Sedimentary section at Purmamarca SP. b. Facies Src, current ripple sandstones, developing double crested ripples. c. Punctuation marks and biological impressions. d. Mud flakes. e. MlRh, laminated rhythmites. f. Palaeocurrent's diagram.

The upper levels of this section record massive and laminated fine sandstones, and laminated mudstones (facies Sl, Sm and MI) with transitional contacts. It ends with 5 m-thick fines and stones with ripple marks of various types (facies Scr). It is characterized by three levels of double-crested ripples associated with wrinkle marks. It includes several levels resembling erosional surfaces to the top of the sequence (Sm) with sub-rounded mud flakes.

Palaeocurrents measured from bidirectional sedimentary structures (double crested ripples) are NE-SW. Unidirectional structures show flux directions towards SE and NW.

Palaeoenvironment evolution.— The basal succession indicates a shallow shelf dominated by wave action in the intertidal nearshore, above the fair-weather wave base. The tractive movement of the sandy material on the flatbed produced vertical aggradation deposits while erosion patterns are evidenced by mud flakes.

The middle section is a tide-dominated shelf dominated by fine material sourced to the basin. The rhythmic graded successions of muddy banks fining upwards with few interbedded storm levels, imply a subtidal, offshore environment. This environment, protected from wave action, has allowed the preservation of the tidal rhythmic sequence. The fine sediments that entered movement during the ebb tides are transported mainly in suspension towards the offshore. These graded rhythmites of tidal origin are correlationable with those from Rancagua and Palermo Oeste SP, and are similar to those of Reynella siltstone, of the Upper Neoproterozoic from South Australia (Williams, 2000).

The upper section shows a lithofacies association that indicates a shallow shelf dominated by tides and waves in the intertidal to subtidal nearshore, above the fair-weather wave base. Intertidal settings are evident from red sediments and associated mud flakes. High flux regime is related to tidal channels (Ch) and linguoid ripples (Src) during ebb. The double-crested ripple marks are typical of tidal environments with asymmetry in ebb and flow currents, and indicate a preferential N-S flux direction.

The lithofacies association allows to interpret the sequence as a tidal flat deposit, in which the biogenic activity has played an important role throughout the entire period of recorded sedimentation. Abundant development of bottom structures, storm layers and exposure levels suggest a position between intertidal to subtidal above the storm wave-base. The tidal regime is characterized by asymmetry of the flood and ebb currents that preferentially followed the basin elongation, and occasionally registered the E-W direction perpendicular to the coastline. The three episodes of subaerial exposure, as well as the presence of a red pelitic bank, suggest a combination of oxidizing conditions in the intertidal setting and erosion of mud cracks and consequent deposition of the mud flakes. This period with high evaporation rates in this profile interchanged with more rainy and

stormy periods (facies HCS) and may correspond to ancient seasonal cycles. The time spans difficult to establish based on the difficulty of knowing with certainty the geologic time recorded in sediment profiles (months, years), especially in those that are ancient.

Considering statements presented by Selley (1968) regarding the three parameters that define a palaeocurrent model, the multidirectional palaeocurrents in Purmamarca SP evidence the following signatures:

- Environment (depositional process): Shallow marine environment characterized by tidal ebb and flood currents, and intertidal environments.
- Azimuthal paleocurrent pattern at outcrop: Bimodal bipolar paleocurrent patterns driven by tractive processes alongshore (double crested ripples) (Figure 9f).
- Relationship between paleocurrents and paleoslope: A NE-ward dipping paleoslope is deduced due to basin configuration and seawater flow and outflow alongshore.

DISCUSSIONS

Considering the early studies on the sedimentation environments of Puncoviscana Formation and interlayered carbonates (Ortíz, 1962; Salfity *et al.*, 1976; Ježek, 1990; Iturriza, 1981; Omarini, 1983; Omarini and Baldis, 1984; Porto *et al.*, 1990), advanced research increased the knowledge of depositional paleoenvironments integrating palaeontological, sedimentological, geochemical and isotopic data (Sial *et al.*, 2001; Aceñolaza and Aceñolaza, 2005; Buatois and Mángano, 2004; Toselli *et al.*, 2005; Aceñolaza and Aceñolaza, 2007; Omarini *et al.*, 2008; López de Azarevich *et al.*, 2010a, d, e, 2012; Escayola *et al.*, 2011; Buatois and Mángano, 2012). From the recognition of rhythmic tidal sequences by López de Azarevich *et al.* (2010a, d), and sedimentary structures formed by bimodal fluxes (López de Azarevich *et al.*, 2010e), a record of shallow marine environments appear to complete the puzzle of marine dynamics within Puncoviscana Formation deposits. Latterly, sequences of Puncoviscana Formation were redefined in localities along West and East margins (Figure 1), and consequently the palaeobathymetric scheme was adjusted for *Nereites* and *Oldhamia* biofacies (review in López de Azarevich *et al.*, 2012) and *Hidrozoa* (Chiliguay *et al.*, 2014, 2016).

The integral analysis of the sedimentological and lithological facies, carbonate geochemistry and paleo-hydrodynamics of the marine fluxes, allow to unravel different aspects on the geologic and hydrodynamic changes throughout the basin evolution. The basin fill initiated with diamictites and turbidites followed by cap carbonates along the eastern margin, and progressed to transgressive deposits up-sequence that covered the whole basin.

Basal successions comprise glacial-derived sediments deposited in agitated, oxidized, shallow marine water (Van Staden and Zimmermann, 2003). The facies analysis and the relatively poor selection and sub-rounded forms of the sedimentary material sourced to the basin suggest that it suffered low rates of transport and re-working by marine processes. This coarse material, transported and deposited by high energy agents, was able to fill the accommodation space generated after the break-up, not as a consequence of sea level rise (Weij *et al.*, 2018), but by buoyancy of the fragmented crustal blocks that led the sea water to penetrate from the north. Asymmetry of the basin topography, fresh water discharge, preferentially located along the eastern margin of the basin, and water hydrodynamics are also interpreted to have conditioned the facies distribution of glacial and post-glacial deposits of Lerma Group.

The post-glacial record for the basin is represented by cap carbonate precipitation, which represents a complete infill of the accommodation space in the eastern margin. Considering the clastic conglomerates that interlayer in the middle succession of the northern carbonate platform, processes of erosion of previous units can be assessed. According to modelling of Alpine Triassic carbonate sequences (Goldhammer *et al.*, 1990), some vertical changes across the larger depositional sequence can be interpreted as differences in the depositional space available during the rising and falling stages of sea-level change. The carbonate sequences pass transitionally towards the fine clastic sedimentites of Puncoviscana Formation, developing a fine interlayering, in both the southern and northern part of the basin (Las Tienditas and Volcán-Tumbaya zones). Such stratigraphic correlation allows to interpret that the platform evolved progressively from carbonate to clastic, similar to an equivalent Brazilian basin (Bambuí Group).

The carbonate geochemistry helps to reinforce that extension was developed above a previous suture zone (Figure 2), which remains from the polycyclic fragmentation and amalgamation of South American cratons and smaller terranes producing the Brasiliano collage (Brito Neves *et al.*, 2014; Rapela *et al.*, 2016). The behaviour of Fe, Al, Mn, Co, Y, V, as well as stable isotopic signatures points towards a chemical precipitation without contribution of hydrothermal fluids and a well mixing of nutrients in sea water. Lack of hydrothermal circulation is evidence that no ocean crust was erupted during the basin evolution, differing from interpretations by Omarini *et al.* (1999), Ramos (2008), Aceñolaza and Toselli (2009), Escayola *et al.* (2011), Hauser *et al.* (2011), Aparicio González (2014), who interpreted an evolution model considering an oceanic crust formation and later subduction that produced the Pampean magmatism (Early Cambrian). In this sense, granite emplacement can occur from other mechanisms such as decompressional melting.

The O and C isotope values in the analysed carbonates are similar to those of other pericontinental basins around Rodinia (Galindo *et al.*, 2004; Misi *et al.*, 2007). The $\delta^{18}\text{O}$ shows oscillation from ~ -10.00 ‰ PDB to -5.3 ‰ PDB that resemble values of Sete Lagoas Formation of Bambuí Group, NE Brazil (Guacaneme *et al.*, 2017). On the other hand, the behaviour of $\delta^{13}\text{C}$ show similarities with the lower section (Linha Verde) of Sete Lagoas Formation. Although Bambuí Group represents an Ediacara-Cambrian marine basin with thicker carbonate deposition, the isotopic data from Sial *et al.* (2001) and from this research shows that different sections of the same unit in Bambuí Group display different $\delta^{18}\text{O}$ vs $\delta^{13}\text{C}$ behaviour (Guacaneme *et al.*, 2017):

- The isotopic signature of Las Tienditas Formation ($\sim +1$ to -2 $\delta^{13}\text{C}$; -5 to -8 $\delta^{18}\text{O}$) is similar to the lower section of Sete Lagoas Formation in the northern part of the basin and also shows some post-depositional evolution. Sete Lagoas Formation evolved from higher to lower $\delta^{18}\text{O}$, whereas Las Tienditas evolved from lower to higher $\delta^{18}\text{O}$.
- The isotopic signature of Tumbaya Formation accompanies that of the upper Sete Lagoas Formation (~ -1.5 to $+3.5$ $\delta^{13}\text{C}$; -11 to -3 $\delta^{18}\text{O}$).
- The isotopic signature of Volcán Formation ($+6$ to $+4.5$ $\delta^{13}\text{C}$; -18 to -8 $\delta^{18}\text{O}$) accompanies that of the Inahúna section from the lower Sete Lagoas Formation, western part of the basin and cap carbonates.

The high consistency in $\delta^{13}\text{C}$ for Volcán Formation can be interpreted as representative of the depositional environment. Moreover, in the lower Sete Lagoas Formation, carbonates with this signature are deposited above the cap carbonates with negative $\delta^{13}\text{C}$ excursion of -4.5 ‰ (Santos *et al.*, 2004; Vieira *et al.*, 2007).

According to Mn/Sr and Fe/Sr ratios and the empirical limits proposed by Fölling and Frimmel (2002) for altered carbonates, the upper section of Las Tienditas profile (Sial *et al.*, 2001) shows evidence of post-depositional alteration possibly related to dolomitization processes and coincides with a decrease of $\delta^{13}\text{C}$ up-sequence and a higher Mg/Ca ratio (Brand and Veizer, 1980). In this profile, $\delta^{18}\text{O}$ shows lower values (-8 ‰) than those from Sete Lagoas (-6.5 to -9.5 ‰) and its behavior against Mn/Sr and Fe/Sr shows a post-depositional alteration trend.

Post-depositional alteration for Lerma Group carbonates were possible due to fluid-rock interactions by fluids with a different oxygen isotopic composition infiltrated the sediment (Banner and Hanson, 1990; Derry, 2010). As no hydrothermal signature was found from carbonate geochemistry, it is possible that the isotopic fractionation of $\delta^{18}\text{O}$ within the platform carbonates were consequence of meteoric water interaction or other regional characteristics such as topography, latitude, altitude, temperature, or evaporation-condensation previous to precipitation (Mook, 2002; Aguilar-Ramírez *et al.*, 2017).

Considering that $^{87}\text{Sr}/^{86}\text{Sr}$ ratios of the carbonates at the base of the deposits (~ 0.7080), are similar to carbonates expected for late Ediacaran (Jacobsen and Kaufman, 1999) and higher up-sequence (~ 0.71017), it is possible that the deposition started in a marine environment with a good connection with open ocean, in which case the Sr isotopic signature equilibrates with the global ocean. Higher values up-sequence indicate a higher contribution of material derived from continental erosion, in which case an increase of continental derived ^{87}Sr would occur (Melezhik *et al.*, 2001) in decrement of marine ^{86}Sr . This situation is in concordance with diminishment of the accommodation space within the basin, restricting the marine flooding and generation of a flat pond with progressively more shallow marine environments of Puncoviscana Formation.

Each SP from Puncoviscana Formation represents the conjunction and special arrangement of several lithofacies, with characteristic shallow sea sedimentary structures and facies associations. Palaeochannels filled with carbonate pebbles immersed in a pelitic matrix (Chiliguay *et al.*, 2019) indicate contribution of the carbonate platform and deposition of eroded material in tidal channels. This process is interpreted as a consequence of sea level lowstands reached by stabilization of buoyancy and produces subaerial exposure.

Tidal flat associations were developed along the West and East margins, clearly recognized in the analysed profiles, and constitute a common assemblage in meso and macrotidal estuaries. The fine material is dominant, and the paleontological registers suggest that biogenic activity played an important role throughout the entire sedimentation rate, producing extended bioturbation. Microbial structures, as well as wave action, were set < 30 m-depth with good oxygenation and illumination by sunlight.

The lithofacies association for Puncoviscana Formation resembles relative increase of sea level and generation of episodically transgressive/regressive facies, and the accommodation/supply balance would occurred in relation with the transgression process (Cattaneo and Steel, 2003, and literature). Consequently, a discontinuous depositional transgression setting can be interpreted. In this scenario the accommodation/supply ratio is always above 1 ($A/S \geq 1$), with low rates of effective deposition and much lower rates of material supplied to the basin, evidencing a rapid sea level rise. In relation to that, Cooper and Pilkey (2004) suggest that the sediment sup-

ply, variations in wave and tide energy, and sediment type, among others, constitute factors causing changes in the morphology of coasts, being the influence of sea-level rise the biggest challenge in discerning the impacts in the shoreline setting. Data evidence that subsidence was not as determinative for lithofacies accumulation as buoyancy driven by changes of the basin topography due to tectonism: granite emplacement along the basin axis that generated water volume displacement toward very low-gradient areas. The rise of the regional base line for continental drainage implied a decrease of the sediment influx to the basin, and together with a tide-dominated setting, helped the cannibalization of previously deposited sediments that could include those deposited in the early stages of transgression. Sediment reworking is the best scenario to generate the very fine, homogenous clastic material of this unit, to which a suspected previous aeolian treatment might be explored for future.

The marine circulation resembles a general north-to-south flooding, with bidirectional/reverse and multidirectional paleocurrents that display bimodal, bipolar and polymodal patterns (Figures 4, 6 and 9). The first ones characterize tidal settings with flood and ebb currents registered in the internal sedimentary structures and bottom morphologies (Src, herringbones, double crested ripples, and asymmetric ripples respectively). The second ones identify the littoral drift along the coasts, generated by a combination of returning currents and winds along the coast. Both hydrodynamic patterns are recorded. As Puncoviscana basin had an N-S elongation, open to the north, the orientation of bimodal-bipolar seawater flux evidence that the configuration of the basin and reversal tidal process played an important role in the hydrodynamics of the environment.

Despite no fluvial deposits are found associated to the basin, and consequently the magnitude of the surficial runoff is uncertain, geochemical signatures and radiometric ages from detrital zircons help in reconstructing the history of the transcontinental drainage sourcing to the basin. Thus the sedimentary sequences of Puncoviscana Formation provide some insights about the palaeotopography and erosional rates throughout the depositional time. The material sourced to the basin by surficial runoff helps the palaeogeographic reconstruction, and emphasizes the role played by rivers in the early life of the basin and its evolution during closure in Early Cambrian. In a similar way, U-Pb studies helped Robinson *et al.* (2014) in deciphering the palaeofluvial and palaeogeographic evolution of the Himalayas. Although Puncoviscana Formation was correlated with metasedimentary sequences outcropping south of Tucumán in Western Sierras Pampeanas, detrital zircon age populations are not coincident in the 1.75 Ga peak, allowing Rapela *et al.* (2016) to discard the Amazonia Craton as the source area for the last sequences. In addition, we interpret two separate ponds developing north and south of Tucumán, formed as pericratonic independent basins around the fragmented Rodinia, in which the different fluvial systems sourcing Puncoviscana Basin (North) can be recognized in the Amazonia-Sunsás

signature. Also, the Zr, Sc and TiO₂ contents, as well as the Zr/Sc vs Th/Sc and Hf vs La/Th behaviour in Puncoviscana Formation (Piñán-Llamas and Escamilla-Casas, 2013) reveal an increased degree of recycling with a clear tendency from the clastic components of the underlying Medina Formation (Figure 2) towards those recorded in Puncoviscana Formation.

Provenance constraints

Considering that the lithosphere in NW Argentina was built-up by the successive accretion of terranes previous to 1 Ga, with the Arequipa-Antofalla terrane (western margin) constituted by several blocks amalgamated during the Sunsás Orogeny at ~1 Ga (Loewy *et al.*, 2004), the paleogeography configuration insert different drainage systems running towards Puncoviscana Sea with zircons belonging to the source areas. Then changes in zircon age populations will accompany the lithofacies changes in the sedimentary sequences.

The ancient orogens of Arequipa-Antofalla (West), Amazonia and the Sunsás Belt (North) and the Pampia Terrain (East), as well as Medina Formation, remained exposed when the deposition of Sancha Formation initiated. By that time, lithofacies distribution indicates a drainage preferentially sourcing from the east and a platform slope gently dipping to the west (Figure 2b-c). Zircon ages of 2.7-2.5 Ga, 2.2-1.8 Ga, 1.2-1.0 Ga and 0.7-0.6 Ga registered by the equivalent Chachapoyas Formation (Table 1), suggest provenance from continental areas in the Amazonia Craton, partially from the Sunsás Belt (Mesoproterozoic), from Late Neoproterozoic orogens of the Brazilian cycle, and from the Pampean magmatism. For Puncoviscana Formation, the detrital zircon age spectra is in the range from 1.9 Ga to 0.5 Ga (Adams *et al.*, 2008; Aceñolaza *et al.*, 2010; Escayola *et al.*, 2011; Aparicio González, 2014). When Alto de la Sierra and Guachos Formations are analysed separately, different source areas suggest a particular evolution regarding the basin dynamics along the Early Cambrian.

In the southern tip of Puncoviscana Formation at Choromoro, zircon populations register mostly Grenville and Pampean ages (Aceñolaza *et al.*, 2010). The rivers sourcing the basin from the south seemed to have collected zircons from Pampia Terrain (southeast), possibly with contributions from Antofalla Terrain (west).

The ancient rivers running from the west towards Rancagua locality (Figure 3) sourced zircons of three population ages: 1.1-0.9 Ga, 0.7-0.6 Ga and 0.53-0.52 Ga (Adams *et al.*, 2008; Aceñolaza *et al.*, 2010). These suggest erosion of the magmatic-metamorphic rocks from Antofalla Terrain (1.5-1.0 Ga, and 0.7-0.6 Ga, Escayola *et al.*, 2011) and contribution from the Tilcara arc. This arc was already active during the depositional time, and represented a barrier for clastic material that could had been transported farther from the east.

In north-eastern Puncoviscana Formation sequences, at Purmamarca and the northern Humahuaca localities (Figure 3), Grenville and Neoproterozoic ages dominate (Aceñolaza *et al.*, 2010), indicating rivers running over Sunsás and Pampia Terranes preferentially. In addition, the time interval of 1.6-1.45 Ga is only registered in Humahuaca locality (Aceñolaza *et al.*, 2010; Escayola *et al.*, 2011). These zircon ages suggest erosion of Archean and Transamazonian terranes that were agglutinated during the Mesoproterozoic (magmatism and metamorphism ages), before the consolidation of the mobile belts and amalgamation of Rodinia (Brasiliano Cycle, Almeida *et al.*, 2000).

From the geotectonic point of view, zircons belonging to the 0.7-0.6 Ga peak indicate the first stage of block accretion and closure of sedimentary basins that conducted to Gondwana amalgamation (Almeida *et al.*, 2000). Zircons of the Alto de la Sierra Formation evidence a very different history than for Puncoviscana Basin configuration. The depositional setting was characterized by a dominant source from Pampean and Tilcara aged landmass (>60% of zircon population, Aparicio González, 2014), which resemble the second and third stages in South American basin closures (Almeida *et al.*, 2000), and the initiation of the magmatic activity along the basin axis, which would produce the elevation of the basin substrate and consequently contributed fluvial valleys to be invaded by sea water. The zircon populations together with this configuration, suggest that neither the sourcing by rivers running over older terranes located north and west nor the reworking of basin material were dominant processes by that time span. Considering this, it is interpreted that basins suffered differential uplift in the southern edge that benefited sourcing from Pampia-aged rocks and produced an out-flooding of sediments towards the north.

Moreover, the upper section of the eastern margin includes also Grenville and Pampean zircons, which suggest slight subsidence of the basin generating the possibility of east and west sourcing from the recycled orogenic material of Pampia and Antofalla Terrains, respectively.

Finally, the paleogeographic configuration of the Middle-Upper Cambrian siliciclastic basin (Mesón Group) copies that of Puncoviscana Basin. Considering that the selection and maturation of clastic material increase from Puncoviscana Formation to the younger Mesón Group successions, changes in platform slope and wave-dominated environment are interpreted for the Middle Cambrian once the Tilcara Orogeny ended.

CONCLUSIONS

Puncoviscana basin represents the latest infilling of a pericontinental foreland marine basin that developed between the Amazonia Craton, the Sunsás Belt, the Arequipa-Antofalla Terrain and the Pampia Terrain, from neoproterozoic to Early Cambrian times. The basal sequence displays post-glacial arrangement and westward sourcing. The overlying Puncoviscana Formation analysed in West and East margins, contain sedimentary structures and facies associations typical of intertidal and subtidal environments with depths not exceeding 30 meters. Diagnostic sedimentary structures evidence reverse and polymodal flux.

The sourced material that contributed to the infill has a provenance from Mesoproterozoic and Neoproterozoic (Grenville and Pampean) landmass located to the East (Amazonia, Sunsás), South (Pampia) and West (Arequipa-Antofalla), as well as from Tilcara magmatic arc (550-511 Ma). The mid-section of Puncoviscana Formation (~545-540 Ma) that includes zircons sourced preferentially from Pampean and Tilcara- aged rocks, allow interpreting a decrease in continental sourcing due to an increase of the relative sea level and hence the baseline of the basin. This is supported by the recycling of clastic material within the basin.

The subsidence of the Puncoviscana Basin was episodic, with changing facies from transgression/regression periods. This is in concordance with zircon ages that register an initial ~25 Ma-episode of active faulting and subsidence (~570-545 Ma) from opening to deposition of the lower section of Puncoviscana Formation, followed by a ~10 Ma-episode of tectonic quiescence (middle section of Puncoviscana Formation) and a final ~20 Ma-episode of tectomagmatic activity that progressed to uplift and closure.

ACKNOWLEDGEMENTS

This research was supported by the Research Project No. 2037 and 2343 with the Consejo de Investigaciones of the Universidad Nacional de Salta (CIUNSa). Authors thank the academic support provided by the CEGA-IN-SUGEO-CONICET, to Dr. Poppe de Boer for suggestions and reviewers' an editorial comments that helped to improve this research.

REFERENCES

- Aceñolaza, F.G. and Toselli, A.J. 2009. The Pampean Orogen: Ediacaran-Lower Cambrian evolutionary history of Central and Northwest region of Argentina. In: Gaucher, C., Sial, A.N., Halverson, G.P. and Frimmel, H. (eds.), Neoproterozoic-Cambrian Tectonics, Global Change and Evolution: a focus on southwestern Gondwana. *Developments in Precambrian Geology* 16, Amsterdam, Elsevier, p. 239-254.

- Aceñolaza, F.G. y Aceñolaza, G.F. 2005. La Formación Puncoviscana y unidades estratigráficas vinculadas en el Neoproterozoico-Cámbrico temprano del noroeste argentino. *Latin American Journal of Sedimentology and Basin Analysis* 12 (2): 65-87.
- Aceñolaza, G.F. and Aceñolaza, G.F. 2007. Insights in the Neoproterozoic / Early Cambrian transition of NW Argentina: facies, environments and fossils in the Proto Margin of Western Gondwana. The Rise and the Fall of the Ediacara Biota. *London, Geological Society of London Special Publication* 286: 1-13.
- Aceñolaza, G.F., Toselli, A.J., Miller, H. and Adams, C. 2010. Interpretación de las poblaciones de circones detríticos en Unidades estratigráficas equivalentes del Ediacarano-Cámbrico de Argentina. In: Aceñolaza, F.G. (ed.), Ediacarano-Cámbrico Inferior Gondwana I. *Serie de Correlación Geológica* 26: 49-64.
- Aguilar-Ramírez, C., Camprubí, A., Fitz-Díaz, E., Cienfuegos-Alvarado, E. and Morales-Puente, P. 2017. Variación en la composición isotópica del agua meteórica a lo largo de la sección centro-noreste de la Sierra Madre Oriental. *Boletín de la Sociedad Geológica Mexicana* 69(2): 447-463.
- Adams, C., Miller, H. and Toselli, A.J. 2008. Detrital zircon U-Pb ages of the Puncoviscana Formation, Late Neoproterozoic – Early Cambrian, of NW Argentina: provenance area and maximum age of deposition. *VI South American Symposium on Isotope Geology (VI SSAGI), Abstracts*, 152.
- Allen, J.R.L. 1968. *Current ripples. Their relation to patterns of water and sediment motion*. North Holland Publ. Co. 433 p.
- Allen, J.R.L. 1984. *Sedimentary structures: their character and physical basis*. Developments in Sedimentology 30, Unabridged One-Volume, 2nd edn. Elsevier, Amsterdam. 1256 pp.
- Almeida, F.F.M., Brito Neves, B.B. and Carneiro, C.D.R. 2000. Origin and evolution of the South American platform. *Earth Science Reviews* 50: 77-111.
- Anderson, T.F. and Raiswell, R. 2004. Sources and mechanisms for the enrichment of highly reactive iron in euxinic Black Sea sediments. *American Journal of Science* 304: 203–233.
- Aparicio González, P.A. 2014. *El basamento estratigráfico (Proterozoico superior-Cámbrico inferior) en la Sierra de Mojotoro, tramo austral de la Cordillera Oriental*. Tesis Doctoral. Universidad Nacional de Salta. 230 pp.
- Aparicio González, P.A., Moya, M.C. e Impiccini, A. 2010. Estratigrafía de las rocas metasedimentarias (Neoproterozoico-Cámbrico) de la Sierra de Mojotoro, Cordillera Oriental, Argentina. *Latin American Journal of Sedimentology and Basin Analysis* 17(2): 65-83.
- Aparicio González, P.A., Pimentel, M.M. and Hauser, N. 2011. Datación U-Pb por LA-ICP-MS de diques graníticos del Ciclo Pampeano, Sierra de Mojotoro, Cordillera Oriental. *Revista de la Asociación Geológica Argentina* 68 (1): 33-38.

- Archer, A.W. 2013. World's highest tides: Hypertidal coastal systems in North America, South America and Europe. *Sedimentary Geology* 284-285: 1-25.
- Banner J.L. and Hanson G.N. 1990. Calculation of simultaneous isotopic and trace element variations during water-rock interaction with application to carbonate diagenesis. *Geochimica et Cosmochimica Acta* 54: 3123-3137.
- Brand U. and Veizer J. 1980. Chemical diagenesis of a multicomponent carbonate system-1: Trace elements. *Journal of Sedimentary Petrology* 50: 1219-1236.
- Bourgeois, J. 1980. A transgressive shelf sequence exhibiting hummocky cross stratification: The Cape Sebastian Sandstone (Upper Cretaceous), southwestern Oregon. *Journal of Sedimentary Petrology* 50: 681-702.
- Brito Neves, B.B. and Fuck, R.A. 2013. Neoproterozoic evolution of the South-American platform. *Journal of South American Earth Sciences* 47: 72-89.
- Brito Neves, B.B., Fuck, R.A. and Pimentel, M.M. 2014. The Brasiliano collage in South America: a review. *Brazilian Journal of Geology* 44(3): 493-518.
- Bryce, S.M., Larcombe, P. and Ridd, P.V. 1998. The relative importance of landward-directed tidal sediment transport versus freshwater flood events in the Norman by River Estuary, Cape York Peninsula. *Marine Geology* 149: 55-78.
- Buatois, L. and Mángano, M.G. 2004. Terminal Proterozoic-Early Cambrian ecosystems: ichnology of the Puncoviscana Formation, northwestern Argentina. *Fossils and Strata* 51: 1-16.
- Buatois, L.A. and Mángano, M.G. 2012. An Early Cambrian shallow-marine ichnofauna from the Puncoviscana Formation of northwest Argentina: the interplay between sophisticated feeding behaviors, matgrounds and sea-level changes. *Journal of Paleontology* 86(1): 7-18.
- Cattaneo, A. and Steel, R.J. 2003. Transgressive deposits: a review of their variability. *Earth-Science Reviews* 62: 187-228.
- Cawood, P.A. 2005. Terra Australis Orogen: Rodinia breakup and development of the Pacific and Iapetus margins of Gondwana during the Neoproterozoic and Paleozoic. *Earth Sciences Reviews* 69: 249-279.
- Chakrabarti, A. 2005. Sedimentary structures of tidal flats: a journey from coast to inner estuarine region of Eastern India. *Journal of Earth Systems Science* 114(3): 353-368.
- Chiliguay, W.J., López de Azarevich, V.L., Zamponi, M. and Azarevich, M.B. 2014. Primer Cnidaria Hydrozoa en ambiente de plataforma en la Formación Puncoviscana (Neoproterozoico-Cámbrico inferior), Jujuy. *XIV Reunión Argentina de Sedimentología, Actas* CD: 81-82.

- Chiliguay, W.J., Zamponi, M., López de Azarevich, V.L. and Azarevich, M.B. 2016. Las anémonas de mar (*Cnidaria-Anthozoa-Actiniaria*) en la Formación Puncoviscana, Jujuy, Argentina. *XXII Congreso Geológico de Bolivia. Actas* CD. 4 pp.
- Chiliguay, W.J., López de Azarevich, V.L., Zamponi, M., Azarevich, M.B. and Muñoz, A. 2019. Paleoambientes de la Formación Puncoviscana (Neoproterozoico – Cámbrico inferior), en el sector oriental de la Quebrada de León, provincia de Jujuy. *Serie de Correlación Geológica* 35(1): 5-26.
- Cooper, J.A.C. and Pilkey, O.H. 2004. Sea-level rise and shoreline retreat: time to abandon the Bruun Rule. *Global and Planetary Change* 43: 157-171.
- Davis, R.A. and Dalrymple, R.W. 2012. *Principles of Tidal Sedimentology*. Springer, New York. 621 pp.
- de Boer, P.L. 1979. Convolute lamination in modern sands of the estuary of the Oosterschelde, the Netherlands, formed as the result of entrapped air. *Sedimentology* 26: 283-294.
- Derry L.A. 2010. A burial diagenesis origin for the Ediacaran Shuram-Wonoka carbon isotope anomaly. *Earth and Planetary Science Letters* 294: 152-162.
- Dott, R.H. and Bourgeois, J. 1982. Hummocky Stratification: Significance of its Variable Bedding Sequences. *Geological Society of America Bulletin* 93(8): 663-680.
- Ehlers, T.A. and Chan, M.A. 1999. Tidal sedimentology and estuarine deposition of the Proterozoic Big Cottonwood Formation, Utah. *Journal of Sedimentary Research* 69(6): 1169-1180.
- Eriksson, P.G., Condie, K.C., Trisgaard, H., Mueller, W.U., Altermann, W., Miall, A.D., Aspler, L.B., Catuneanu, O. and Chiarenzelli, J.R. 1998. Precambrian clastic sedimentation systems. *Sedimentary Geology* 120 (1-4): 5-53.
- Escayola, M.P., van Staal, C.R. and Davis, W.J. 2011. The age and tectonic setting of the Puncoviscana Formation in northwestern Argentina: An accretionary complex related to Early Cambrian closure of the Puncoviscana Ocean and accretion of the Arequipa-Antofalla block. *Journal of South American Earth Sciences* 32: 438-459.
- Fike, D.A., Grotzinger, J.P., Pratt, L.M. and Summons, R.E. 2006. Oxidation of the Ediacaran Ocean. *Nature* 444: 67-87.
- Fölling P.G. and Frimmel H.E. 2002. Chemostratigraphic correlation of carbonate successions in the Gariiep and Saldania Belts, Namibia and South Africa. *Basin Research* 14: 69-88.
- Font, E., Nédélec, A., Trindade, R.I.F., Macouin, M. and Charrière, A. 2006. Chemostratigraphy of the Neoproterozoic Mirassol d'Oeste cap dolostones (Mato Grosso, Brazil): An alternative model for Marinoan cap dolostone formation. *Earth and Planetary Science Letters* 250: 89-103.

- Galindo, C., Casquet, C., Rapela, C., Pankhurst, R.J., Baldo, E. and Saavedra, J. 2004. Sr, C and O isotope geochemistry and stratigraphy of Precambrian and lower Paleozoic carbonate sequences from the Western Sierras Pampeanas of Argentina: tectonic implications. *Precambrian Research* 131: 55-71.
- Ginsberg, S.S., Aliotta, S. and Lizasoain, G.O. 2009. Sistema interconectado de canales de marea del estuario de Bahía Blanca, Argentina: evaluación de la circulación de sedimento como carga de fondo por métodos acústicos. *Latin American Journal of Aquatic Research* 37(2): 231-245.
- Goldhammer, R.K., Dunn, P.A. and Hardie, L.A. 1990. Depositional cycles, composite sea-level changes, cycle stacking patterns, and the hierarchy of stratigraphic forcing: Examples from Alpine Triassic platform carbonates. *GSA Bulletin* 102(5): 535-562.
- Guacaneme, C., Babinski, B., de Paula-Santos, G. and Pedrosa-Soares, A. 2017. C, O, and Sr isotopic variations in Neoproterozoic-Cambrian carbonate rocks from Sete Lagoas Formation (Bambuí Group), in the Southern São Francisco Basin, Brazil. *Brazilian Journal of Geology* 47(3): 521-543.
- Guidi, R., Mas, R. and Sarti, G. 2005. La sucesión sedimentaria siliciclástica del Cretácico superior del borde sur de la Sierra de Guadarrama (Madrid, España central): análisis de facies y reconstrucción paleoambiental. *Revista de la Sociedad Geológica de España* 18(1-2): 99-111.
- Halverson, G.P., Hurtgen, M.T., Porter, S.M. and Collins, A.S. 2009. Neoproterozoic-Cambrian Biogeochemical Evolution. In: Gaucher, C., Sial, A.N., Halverson, G.P., Frimmel, H.E. (Eds.): Neoproterozoic-Cambrian Tectonics, Global Change and Evolution: a focus on southwestern Gondwana. *Developments in Precambrian Geology* 16: 351-365.
- Harms, J.C., Southard, J.B., Spearing, D.R. and Walker, R.G. 1975. Depositional environments as interpreted from primary sedimentary structures and stratification sequences. *Society of Economic, Paleontology and Mineralogy*, Short Course 2. Dallas.
- Harms, J.C., Southard, J.B. and Walker, R.G. 1982. Structure and sequences in clastic rocks. Lecture Notes: *Society of Economic, Paleontology and Mineralogy*, Short Course 9. Calgary.
- Hauser, N. 2011. *Petrología y geología isotópica de las rocas ígneas y estudios de proveniencia (U-Pb y Lu-Hf) de las rocas metasedimentarias del basamento del Paleozoico inferior en las áreas de Tastil, Niño Muerto, Río Blanco y Río Grande, Cordillera Oriental, noroeste argentino*. Tesis Doctoral. Universidad Nacional de Salta. 330 p.
- Hauser, N., Matteini, M., Omarini, R.H. and Pimentel, M.M. 2011. Combined U-Pb and Lu-Hf isotope data on turbidites of the Paleozoic basement of NW Argentina and petrology of associated igneous rocks: implications for the tectonic evolution of western Gondwana between 560 and 460 Ma. *Gondwana Research* 19(1): 100-127.

- Hjulstrom, F. 1935. Studies of the morphological activity of rivers as illustrated by the River Fyris. *Bulletin of the Geological Institute* 25: 221-527. Upsala.
- Hongn, F.D., Tubía, J.M., Aranguren, A. and Mon, R. 2001. El batolito de Tastil (Salta, Argentina): un caso de magmatismo poliorogénico en el basamento andino. *Boletín Geológico y Minero* 112(3): 113-124.
- Houseman, G.A. 1990. The thermal structure of mantle plumes: axisymmetric or triple junction? *Geophysical Journal International* 102: 15-20.
- Huang, J., Chu, X., Jiang, G., Feng, L. and Chang, H. 2011. Hydrothermal origin of elevated iron, manganese and redox-sensitive trace elements in the c. 635 Ma Doushantuo cap carbonate. *Journal of the Geological Society* 168: 805-815.
- Iturriza, R. 1981. *Perfil geológico del Arroyo Los Noques, Sierra de Castillejo – Dpto Capital-Salta*. Tesis Profesional. Universidad Nacional de Salta. 77 pp.
- Ježek, P. 1990. Análisis sedimentológico de la Formación Puncoviscana entre Tucumán y Salta. En: Aceñolaza, F.G., Miller H., Toselli A.J. (Eds), El Ciclo Pampeano en el noroeste argentino. *Serie de Correlación Geológica* 4: 9-36.
- Jacobsen S.B. and Kaufman A.J. 1999. The Sr, C and O isotopic evolution of Neoproterozoic seawater. *Chemical Geology* 161: 37-57.
- Johnson, H.D. and Baldwin, C.T. 1996. *Shallow clastic seas*. In: Sedimentary Environments: Processes, Facies and Stratigraphy, 3rd edn (Ed. Reading, H.G.), pp. 232-280. Blackwell Science, Oxford.
- Keppie, J. and Bahlburgh, H. 1999. Puncoviscana Formation of northwestern and central Argentina: passive margin or foreland basin deposit. In: V.A. Ramos, J.D. Keppie (Eds.), Laurentia-Gondwana connections before Pangea. *Geological Society of America Special Paper* 336: 139-143.
- Kraemer, P.E., Escayola, M.P. and Martino, R.D. 1995. Hipótesis sobre la evolución tectónica neoproterozoica de las Sierras Pampeanas de Córdoba (30°40'-32°40'), Argentina. *Revista de la Asociación Geológica Argentina* 50: 47-59.
- Kuchenbecker, M., Babinski, M., Pedrosa-Soares, A., Lopes-Silva, L. and Pimenta, F. 2016. Chemostratigraphy of the lower Bambuí Group, southwestern São Francisco Craton, Brazil: insights on Gondwana paleoenvironments. *Brazilian Journal of Geology* 46(1): 145-162.
- Longhitano, S.G., Mellere, D., Steel, R.J. and Ainsworth, R.B. 2012. Tidal depositional systems in the rock record: A review and new insights. *Sedimentary Geology* 279: 2-22.
- López, V., Argañaraz, R., López Ogalde, N. and Azarevich, M. 2006. El basamento calcáreo de la Sierra de Castillejo: caracterización petrográfica y geoquímica. *XI Congreso Geológico Chileno. Actas*: 73-76. Antofagasta.

- López de Azarevich, V.L. 2010. Advances in harmonic analysis of tidal rhythmites in the Puncoviscana Formation (Proterozoic – Early Cambrian), northwest Argentina. *18^o International Sedimentological Congress, Abstract 606*. Mendoza.
- López de Azarevich, V.L. and Azarevich, M.B. 2015a. Exploring the evolving earth from tidal rhythmicity and lunar retreat. *Tidalites 2015. 9^o International Conference on Tidal Sedimentology. Actas: 54-57*. Puerto Madryn, Argentina.
- López de Azarevich, V.L. and Azarevich, M.B. 2015b. Neoproterozoic – Early Cambrian tidal deposits of Northwestern Argentina. *Tidalites 2015. 9^o International Conference on Tidal Sedimentology. Actas: 99-102*. Puerto Madryn, Argentina.
- López de Azarevich, V.L. and Azarevich, M.B. 2017. Lunar recession encoded in tidal rhythmites: a selective overview with examples from Argentina. *Geomarine Letters 37*: 333-344.
- López de Azarevich, V.L., Omarini, R.H., Sureda, R.J. and Azarevich, M.B. 2010a. Ritmitas mareales en la Formación Puncoviscana (s.l.), en la localidad de Rancagua, noroeste argentino: dinámica mareal y consideraciones paleoastronómicas. *Revista de la Asociación Geológica Argentina 66* (1): 104-118.
- López de Azarevich, V.L., Omarini, R.H., Santos, R., Azarevich, M.B. and Sureda, R.J. 2010b. Nuevos aportes isotópicos para secuencias carbonáticas del Precámbrico superior (Formación Las Tienditas) del NO de Argentina: su implicancia en la evolución de la Cuenca Puncoviscana. En: Aceñolaza, F.G. (Ed.), *Ediacarano-Cámbrico Inferior Gondwana I. Serie de Correlación Geológica 26*:27-48.
- López de Azarevich, V.L., Aceñolaza, F.G., Azarevich, M.B. and Omarini, R.H. 2010c. Estructuras microbiales y algales de zona fótica en la Formación Puncoviscana, provincia de Salta, Argentina. En: Aceñolaza, F.G. (Ed.), *Ediacarano-Cámbrico Inferior Gondwana I. Serie de Correlación Geológica 26*: 75-84.
- López de Azarevich, V.L., Azarevich, M.B. and Omarini, R.H. 2010d. Nuevas metodologías aplicadas al estudio de secuencias sedimentarias de plataforma en el basamento Ediacarano-Cámbrico inferior del NO argentino (Formación Puncoviscana). En: Aceñolaza, F.G. (Ed.), *Ediacarano-Cámbrico Inferior Gondwana I. Serie de Correlación Geológica 26*: 103-120.
- López de Azarevich, V.L., Archer, A.W., Omarini, R.H. and Azarevich, M.B. 2010e. Sedimentary structures in the Puncoviscana Formation (Proterozoic - Early Cambrian), NW-Argentina: a comparison with modern shallow water analogs. *18^o International Sedimentological Congress, Abstract 652*. Mendoza.

- López de Azarevich, V.L., Aceñolaza, F.G., Aceñolaza, G.F., Omarini, R.H. and Azarevich, M.B. 2012. La cuenca neoproterozoica-eocámbrica en el NOA: sedimentología y ambientes de depósito de secuencias con icnofósiles, nuevas perspectivas. En: Marquillas, R.A., Sánchez, M.C., Salfity J.A. (Eds.), *Relatorio XIII Reunión Argentina de Sedimentología*: pp 119-132. Salta. ISBN 978-987-26890-1-8.
- Loewy, S.L., Connelly, J.N. and Dalziel, I.W.D. 2004. An orphaned basement block: The Arequipa-Antofalla Basement of the central Andean margin of South America. *GSA Bulletin* 116(1, 2): 171-187.
- Lyons, T.W. and Severmann, S. 2006. A critical look at iron paleoredox proxies: New insights from modern euxinic marine basins. *Geochimica et Cosmochimica Acta* 70: 5698-5722.
- Mazumder, R. and Arima, M. 2005. Tidal rhythmites and their implications. *Earth-Science Reviews* 69: 79-95.
- Melezhik, V., Gorokhov, I., Kuznetsov, A. and Fallick, A. 2001. Chemostratigraphy of Neoproterozoic carbonates: implications for 'blind dating'. *Terra Nova* 13: 1-11.
- Middleton, G.V. and Southard, J.B. 1984. Mechanisms of sediment movement. *Society of Economic, Paleontology and Mineralogy*, Short Course 3. Tulsa.
- Misi, A., Kaufman, A., Veizer, J., Powis, K., Azmy, K., Boggiani, Gaucher, C., Teixeira, J., Sanches, A. and Iyer, S. 2007. Chemostratigraphic correlation of Neoproterozoic successions in South America. *Chemical Geology* 237: 143-167.
- Mook, W.G. 2002. Isótopos ambientales en el ciclo hidrológico, principios y aplicaciones: *Publicaciones del Instituto Geológico y Minero de España*, Serie: Guías y manuales, 1: 595 p.
- Mon, R. and Hongn, F.D. 1991. The structure of the Precambrian and Lower Paleozoic Basement of the Central Andes between 22° and 32°S Lat. *Geologische Rundschau* 80(3): 745-758.
- Mon, R. and Hongn, F.D. 1996. Estructura del basamento proterozoico y paleozoico inferior del norte argentino. *Revista de la Asociación Geológica Argentina* 51(1): 3-14.
- Nichols, G. 2009. *Sedimentology and Stratigraphy*. Second Edition. Blackwell, John Wiley & Sons, Ltd., Publication, UK. 419 pp.
- Nofke, N. 2010. *Microbial Mats in Sandy Deposits from the Archean Era to Today*. Springer, New York. 177 pp.
- Omarini, R.H. 1983. *Caracterización litológica, diferenciación y génesis de la Formación Puncoviscana entre el Valle de Lerma y la Faja Eruptiva de la Puna*. Tesis Doctoral. Universidad Nacional de Salta. 202 p.
- Omarini, R.H. and Baldis, B.A. 1984. Sedimentología y mecanismos deposicionales de la formación Puncoviscana (Grupo Lerma, Precámbrico-Cámbrico) del noroeste argentino. *9° Congreso Geológico Argentino, Acta* 1: 384-398, S. C. Bariloche.

- Omarini, R.H., Torres, G. and Moya, L. 1996. El stock Tipayoc: genesis magmática en un arco de islas del Cámbrico inferior en noroeste de Argentina. *13° Congreso Geológico Argentino, Actas* 5: 545-561.
- Omarini, R.H., Sureda, R.J., Götze, H., Seilacher, A. and Pflüger, F. 1999. Puncoviscana folded belt in northwestern Argentina: testimony of Late Proterozoic Rodinia fragmentation and pre-Gondwana collisional episodes. *International Journal of Earth Science* 88: 76-97.
- Omarini, R.H., Sureda, R.J., López de Azarevich, V.L. and Hauser, N. 2008. El basamento Neoproterozoico-Cámbrico inferior en la provincia de Jujuy. En: Coira, B., Zappettini, E. (Eds.), *Geología y Recursos Naturales de la provincia de Jujuy*. Relatorio XVII Congreso Geológico Argentino, Chapter IIa: Ciclo Pampeano y Famatiniano 17-28.
- Ortíz, A. 1962. *Estudio geológico de las Sierras de Castillejo y Sancha*. Tesis Doctoral. Universidad Nacional de Tucumán.
- Pettijohn, F.J. 1975. *Sedimentary rocks*. Harper and Row, New York. 628 pp.
- Pettijohn, F.J. and Potter, P.E. 1964. *Atlas and glossary of primary sedimentary structures*. Springer-Verlag, New York, USA. 370 pp.
- Piñán-Llamas, A. and Escamilla-Casas, J.C. 2013. Provenance and tectonic setting of Neoproterozoic to Early Cambrian metasedimentary rocks from the Cordillera Oriental and Eastern Sierras Pampeanas, NW Argentina. *Boletín Sociedad Geológica Mexicana* 65(2): 373-395.
- Porto, J.C., Fernández, R. and Carrión, M.H. 1990. Dolomías de la Formación Puncoviscana s.l. En: Aceñolaza, F.G., Miller, H., Toselli, A.J. (Eds.), *El Ciclo Pampeano en el Noroeste Argentino. Serie de Correlación Geológica* 4: 37-52.
- Press, F. and Siever, R. 1986. *Earth* (2nd edition). W.H. Freeman, New York, 649 pp.
- Ramos, V.A. 2008. The basement of the central Andes: the Arequipa and related terranes. *Annual Review of Earth and Planetary Sciences* 36: 289-324.
- Rapela, C.W., Verdecchia, S.O., Casquet, C., Pankhurst, R.J., Baldo, E.G., Galindo, C., Murra, J.A., Dahlquist, J.A. and Fanning, C.M. 2016. Identifying Laurentian and SW Gondwana sources in the Neoproterozoic to Early Paleozoic metasedimentary rocks of the Sierras Pampeanas: Paleogeographic and tectonic implications. *Gondwana Research* 32: 193-212.
- Ross, R.J. 1991. Tectonic setting in the Windermere Supergroup: The continental perspective. *Geology* 19: 1125-1128.
- Robinson, R.A.J., Brezina, C.A., Parrish, R.R., Horstwood, M.S.A., Oo, A.W., Bird, M.I., Thein, M., Walters, A.S., Oliver, G.J.H. and Zaw, K. 2014. Large rivers and orogens: The evolution of the Yarlung Tsangpo–Irrawaddy system and the eastern Himalayan syntaxis. *Gondwana Research* 26: 112-121.

- Salfity, J.A., Omarini, R., Baldis, B. and Gutierrez, W. 1976. Consideraciones sobre la evolución geológica del Precámbrico y Paleozoico del norte argentino. *2º Congreso Iberoamericano de Geología Económica, Actas 4*: 341-361. Buenos Aires.
- Sankaran, A.V. 2000. Global icecover—A Neoproterozoic puzzle. *Global ice cover – A Neoproterozoic puzzle. Current Science 79(3)*: 274-277.
- Santos, R.V., Alvarenga, C.J.S., Babinski, M., Ramos, M.L.S, Cukrov, N., Fonseca, M.A., Sial, A.N., Dardenne, M.A. and Noce, C.M. 2004. Carbon isotopes of Mesoproterozoic–Neoproterozoic sequences from Southern São Francisco craton and Araçuaí Belt, Brazil: Paleogeographic implications. *Journal of South American Earth Sciences 18*: 27-39.
- Scholle, P.A. and Arthur, M.A. 1980. Carbon isotope fluctuations in Cretaceous pelagic limestones potential stratigraphic and petroleum exploration tool. *American Association of Petroleum Geology Bulletin 64*: 67-87.
- Selley, R.C. 1968. A classification of paleocurrent models. *Journal of Geology 76(1)*: 99-110.
- Sial, A., Ferreira, V., Dealmeida, A., Romano, A., Parente, C., Dacosta, M. and Santos, V. 2000. Carbon isotope fluctuations in Precambrian carbonate sequences of several localities in Brazil. *Anais Academia Brasileira Ciencia 72(4)*: 539-558.
- Sial, A.N., Ferreira, V.P., Toselli, A.J., Aceñolaza, F.G., Pimentel, M.M., Parada, M.A. and Alonso, R.N. 2001. C and Sr isotopic evolution of carbonate sequences in NW Argentina: implications for a probable Precambrian-Cambrian transition. *Carbonates and Evaporites 16(2)*: 141-152.
- Silva, L.C., McNaughton, N.J., Armstrong, R., Hartmann, L.A. and Fletcher, I.R. 2005. The Neoproterozoic Mantiqueira Province and its African connections: a zircon-based geochronological subdivision for the Brasiliano/Pan-African system of orogens. *Precambrian Research 136*: 203-240.
- Storey, B., Alabaster, T., Macdonald, D., Pankhurst, R. and Dalziel, I. 1992. Upper Proterozoic rift-related rocks in the Pensacola Mountains, Antarctica: precursors to supercontinent breakup?. *Tectonics 11*: 1392–1405.
- Sureda, R.J. and Omarini, R.H. 1999. Evolución geológica y nomenclatura pre-Gondwánica en el Noroeste de Argentina (1800-160 Ma). *Acta Geológica Hispánica 34(2-3)*: 197-225.
- Tapia Viedma, S. and Gorustovich, S. 1998. Estudio Geológico y ubicación de las calizas negras (Formación Las Tienditas) de El Coro, Salta. *VII Congreso Argentino de Geología Económica, Actas 2*: 111-116.
- Toselli, A.J., Aceñolaza, F.G., Sial, A.N., Rossi, J.N., Ferreira V.P. and Alonso, R.N. 2005. Rocas carbonáticas de la Formación Puncoviscana en las Provincias de Salta y Jujuy, norte de Argentina. *16º Congreso Geológico Argentino, Actas 4*: 647-652, La Plata.

- Turner, J.C.M. 1960. Estratigrafía de la Sierra de Santa Victoria y adyacentes. *Boletín de la Academia Nacional de Ciencias* 41 (2): 163-196, Córdoba.
- Van Staden, A. and Zimmermann, U. 2003. Tillites or ordinary conglomerates? Provenance studies on diamictites of the Neoproterozoic Puncoviscana in NW Argentina. *10° Congreso Geológico Chileno, Abstract Volume. CD*. Concepción.
- Vieira L.C., Trindade R.I.F, Nogueira A.C.R. and Ader M. 2007. Identification of a Sturtian cap carbonate in the Neoproterozoic Sete Lagoas carbonate platform, Bambuí Group, Brazil. *Comptes Rendus Geoscience* 339: 240-258.
- Vos, R.G. and Erikson, K.A. 1977. An embayment model for tidal and wave swash deposits occurring within a fluviially dominated middle Proterozoic sequence in South Africa. *Sedimentary Geology* 18: 161-173.
- Walker, R.G. and Plint, A.G. 1992. Wave- and storm-dominated shallow marine systems. In: Walker R.G., James N.P. (Eds.), *Facies models: Response to sea level change*, pp. 219-238. Geological Association of Canada, St John's Newfoundland.
- Weij, R., Reijmer, J.J., Eberli, G.P. and Swart, P.K. 2018. The limited link between accommodation space, sediment thickness, and inner platform facies distribution (Holocene-Pleistocene, Bahamas). *The Depositional Record* 2018: 1-21. doi: 10.1002/dep2.50.
- Williams, G.E. 1991. Upper Proterozoic tidal rhythmites, South Australia: sedimentary features, deposition, and implications for the Earth's palaeorotation. In: Smith, A., Reinson, G.E., Zaitlin B.A., Rahmani, R.A. (Eds.), *Clastic Tidal Sedimentology. Canadian Society Petroleum Geologists Memories* 16: 161-177.
- Williams, G.E. 2000. Geological constraints on the Precambrian history of Earth's rotation and the Moon's orbit. *Reviews of Geophysics* 38: 37-59.
- Young, G.M. 2013. Precambrian supercontinents, glaciations, atmospheric oxygenation, metazoan evolution and an impact that may have changed the second half of Earth history. *Geoscience Frontiers* 4: 247-261.
- Zimmermann, U. 2005. Provenance studies of very low- to low-grade metasedimentary rocks of the Puncoviscana complex, northwest Argentina. In: Vaughan, A.P.M., Leat P.T., Pankhurst R.J (Eds.), *Terrane Processes at the Margins of Gondwana. Geological Society of London, Special Publication* 246: 381-416.